

Lawrence Berkeley National Laboratory

Lawrence Berkeley National Laboratory

Title

Parametric Evaluation of an Innovative Ultra-Violet Photocatalytic Oxidation (UVPCO) Air Cleaning Technology for Indoor Applications

Permalink

<https://escholarship.org/uc/item/5c35c2pf>

Authors

Hodgson, Alfred T.
Sullivan, Douglas P.
Fisk, William J.

Publication Date

2005-10-31

Parametric Evaluation of an Innovative Ultra-Violet Photocatalytic Oxidation (UVPCO) Air Cleaning Technology for Indoor Applications

Alfred T. Hodgson, Douglas P. Sullivan, and William J. Fisk

Indoor Environment Division, Environmental Energy Technologies Division, E.O. Lawrence Berkeley National Laboratory, Berkeley, CA, USA

October 31, 2005

Abstract

An innovative Ultra-Violet Photocatalytic Oxidation (UVPCO) air cleaning technology employing a semitransparent catalyst coated on a semitransparent polymer substrate was evaluated to determine its effectiveness for treating mixtures of volatile organic compounds (VOCs) representative of indoor environments at low, indoor-relevant concentration levels. The experimental UVPCO contained four 30 by 30-cm honeycomb monoliths irradiated with nine UVA lamps arranged in three banks. A parametric evaluation of the effects of monolith thickness, air flow rate through the device, UV power, and reactant concentrations in inlet air was conducted for the purpose of suggesting design improvements.

The UVPCO was challenged with three mixtures of VOCs. A synthetic office mixture contained 27 VOCs commonly measured in office buildings. A building product mixture was created by combining sources including painted wallboard, composite wood products, carpet systems, and vinyl flooring. The third mixture contained formaldehyde and acetaldehyde. Steady state concentrations were produced in a classroom laboratory or a 20-m³ chamber. Air was drawn through the UVPCO, and single-pass conversion efficiencies were measured from replicate samples collected upstream and downstream of the reactor. Thirteen experiments were conducted in total.

In this UVPCO employing a semitransparent monolith design, an increase in monolith thickness is expected to result in general increases in both reaction efficiencies and absolute reaction rates for VOCs oxidized by photocatalysis. The thickness of individual monolith panels

was varied between 1.2 and 5 cm (5 to 20 cm total thickness) in experiments with the office mixture. VOC reaction efficiencies and rates increased with monolith thickness. However, the analysis of the relationship was confounded by high reaction efficiencies in all configurations for a number of compounds. These reaction efficiencies approached or exceeded 90% for alcohols, glycol ethers, and other individual compounds including d-limonene, 1,2,4-trimethylbenzene, and decamethylcyclopentasiloxane. This result implies a reaction efficiency of about 30% per irradiated monolith face, which is in agreement with the maximum efficiency for the system predicted with a simulation model. In these and other experiments, the performance of the system for highly reactive VOCs appeared to be limited by mass transport of reactants to the catalyst surface rather than by photocatalytic activity.

Increasing the air flow rate through the UVPCO device decreases the residence time of the air in the monoliths and improves mass transfer to the catalyst surface. The effect of gas velocity was examined in four pairs of experiments in which the air flow rate was varied from approximately 175 m³/h to either 300 or 600 m³/h. Increased gas velocity caused a decrease in reaction efficiency for nearly all reactive VOCs. For all of the more reactive VOCs, the decrease in performance was less, and often substantially less, than predicted based solely on residence time, again likely due to mass transfer limitations at the low flow rate. The results demonstrate that the UVPCO is capable of achieving high conversion efficiencies for reactive VOCs at air flow rates above the base experimental rate of 175 m³/h.

The effect of UV power was examined in a series of experiments with the building product mixture in which the number of lamps was varied between nine and three. For the most reactive VOCs in the mixture, the effects of UV power were surprisingly small. Thus, even with only one lamp in each section, there appears to be sufficient photocatalytic activity to decompose most of the mass of reactive VOCs that reach the catalyst surface. For some less reactive VOCs, the trend of decreasing efficiency with decreasing UV intensity was in general agreement with simulation model predictions.

The UVPCO device easily decomposed formaldehyde. At an air flow rate near 300 m³/h, the reaction efficiency was about 60%. There was no apparent effect on conversion of formaldehyde concentration in the range of 24 to 88 ppb. However, the reaction efficiency was about 40 – 50% higher than predicted based on unreported experiments conducted at 1 ppm.

Formaldehyde, acetaldehyde, and acetone were produced as reaction products in these experiments. Overall, about 22% of the carbon introduced into the device was converted to these products instead of completely oxidizing to carbon dioxide. Acetone, a compound with relatively low toxicity, comprised about 60% of the products formed. In experiments with the office VOC mixture there was substantial formation of acetaldehyde and low net formation of formaldehyde. The mixture contained ethanol, a likely reactant leading to acetaldehyde formation. In experiments with the building product mixture, both formaldehyde and acetaldehyde were formed. The design of a UVPCO device for use in occupied buildings needs to minimize the formation of these two unwanted byproducts as they are considered to be carcinogens and have relatively low exposure guidelines for noncancer effects.

INTRODUCTION

Photocatalytic reactions to decompose organic compounds utilize ultra-violet light to activate a semiconductor material. Absorbed photons create an electron-hole pair within the semiconductor. The reducing electron reacts with oxygen while the oxidizing hole reacts with water, creating hydroxyl radicals thought to be responsible for decomposition of organic compounds bound to the surface of the semiconductor. Ideally, only carbon dioxide and water are produced. The earliest work on ultra-violet photocatalytic oxidation (UVPCO) was with aqueous systems. However, gas-phase heterogeneous UVPCO technology, in various forms, has been under investigation for over 20 years. Based on early, published data of oxidation rates for volatile organic compounds (VOCs), a large class of indoor air gaseous contaminants, Henschel (1998) published a comparison of costs for treatment of indoor air by UVPCO versus treatment with granular activated carbon (GAC). In this analysis, the estimated costs for UVPCO were unfavorable with respect to GAC. But, there have been continuing advances in UVPCO technology plus changes in energy, waste disposal, and other costs suggesting that this economic analysis may be outdated.

UVPCO air cleaning technology appears to be generating renewed interest with respect for removal of gas-phase organic contaminants from air in occupied environments including residences, office buildings, aircraft cabins. In particular, UVPCO is potentially well suited for use in large commercial buildings, such as office and retail buildings where the major indoor-generated air pollutants of concern with respect to occupant health and comfort are believed to

be gaseous VOCs and particles of various types. If UVPCO can be implemented successfully in such buildings to reduce concentrations of VOCs, it may be possible when combined with improved particle filtration, to reduce the supply of outdoor air without degrading indoor air quality. Such a reduction in ventilation requirements with concomitant energy savings and reductions in peak power consumption makes UVPCO a potentially attractive energy-conservation technology.

UVPCO is the subject of a recent comprehensive literature review (Zeltner and Tompkins, 2005; Tompkins et al., 2005a and 2005b) that includes descriptions of the photocatalytic process, reaction mechanisms, factors affecting reaction rates, kinetic modeling, economics, and utilization. This review reveals that approximately 40 individual organic compounds relevant to indoor environments have been studied in heterogeneous gas-phase photocatalytic oxidation (Tompkins et al., 2005a). A few of these compounds, such as ethanol, toluene, benzene, trichloroethene, and formaldehyde, have been the subject of numerous investigations. The large majority of the investigations has utilized bench-scale reactors and has employed relatively high concentrations of a few VOCs often in an attempt to better understand the photocatalytic process and to improve various aspects of the technology. We found only one published study, in which an attempt was made to remove VOCs from indoor air in an ordinary room (Disdier et al., 2005). But, the details of the reactor and the experiment are incomplete, and results only are shown for formaldehyde, acetaldehyde and acetone.

Tompkins et al. (2005a) contend the primary challenges to the commercialization of UVPCO for building applications are to design devices that have low pressure drop, use light efficiently, employ catalysts that can readily be regenerated if they become poisoned or deactivated, and don't generate harmful byproducts at levels of concern. Their conclusions include recommendations that research be conducted to investigate: a) low-level concentrations of VOCs that are representative of indoor environments; b) the use of UVPCO in airstreams with typical mixtures of pollutants; and c) the potential formation of reaction by-products. Such studies are a prerequisite for determining the feasibility of employing the technology as a means of reducing outdoor air ventilation requirements in large buildings.

Formation of unwanted byproducts is a potential impediment to the development of UVPCO technologies for indoor air applications. In some of the reviewed studies, Tompkins et

al. (2005a) noted the production of reaction products or intermediates, including formaldehyde, acetaldehyde, formic acid, and acetic acid. Recent studies have detected the same compounds. Chen et al. (2005) identified acetic acid as an oxidation byproduct when a UVPCO was operated with a challenge mixture of 17 VOCs. Disdier et al. (2005) showed small increases in the concentrations of formaldehyde, acetaldehyde, and acetone due to the operation of a UVPCO device in a room. Ginestet et al. (2005) evaluated various UVPCO configurations for potential aircraft cabin applications. When challenged with 10 ppm toluene, acetone, or ethanol, the device operated in single-pass mode produced about 40 – 60 ppb formaldehyde; ethanol resulted in a 1.7-ppm downstream acetaldehyde concentration.

The potential formation of phosgene from the photocatalytic oxidation of trichloroethene has generated considerable interest. The issue was studied in detail by Jacoby et al. (1994). These researchers used a gas-phase Fourier transform infrared spectrometer to identify and quantify intermediates and products and to provide carbon and chlorine mass balances for experiments with a small titania photocatalytic reactor. Dichloroacetyl chloride, phosgene, and hydrogen chloride were observed in the effluent stream. Alberici et al. (1998) utilized on-line mass spectrometry to identify gas-phase by products of the oxidation of trichloroethene, tetrachloroethene, chloroform and dichloromethane. Phosgene, dichloroacetyl chloride, and trichloroacetyl chloride were detected as by-products in some of these experiments. Fortunately, the use of halogenated solvents is in decline and the indoor concentrations of trichloroethene and other chlorinated solvents in office buildings and residences appear to have decreased in recent years to generally low levels (Hodgson and Levin, 2003).

UVPCO technologies often utilize a honeycomb configured, opaque monolith reactor coated with titanium dioxide (TiO_2 or titania) as the photo-oxidative catalyst. This general monolith configuration potentially can have high conversion rates with low pressure drop making it suitable for use in building heating, ventilating and air conditioning (HVAC) systems. However because the monolith is opaque, direct irradiation of the honeycomb surfaces is subject to a shadowing effect of the passage walls (Khalifa, 2005). The UVPCO technology evaluated in the current study differs from this conventional design in that it employs a patented semitransparent photocatalytic/barrier coating on a semitransparent polymer substrate developed by Titan Technologies (Sebastopol, CA). The honeycomb monolith structure is retained for reasons of minimizing pressure drop while providing acceptable mass transfer characteristics.

This technology is suggested to yield improved performance, compared to an opaque system, by allowing 365 nm UV light to penetrate into the monolith structure. Since the reaction order for photocatalysis has been shown to be less than unity in a system not limited by mass transfer, distributing a given amount of light over a larger surface in a semitransparent system should result in a gain in net reaction efficiency if the photocatalytic activities of the semitransparent and opaque catalysts are comparable.

This study was conducted with the primary objective of measuring the effectiveness of Titan Technologies' semitransparent photocatalytic technology for decomposing mixtures of VOCs representative of indoor environments at low, indoor-relevant concentration levels. A parametric evaluation of the effects of monolith thickness, air flow rate through the device, UV power, and reactant concentrations in inlet air was conducted for the purpose of suggesting design improvements. We also investigated the formation of gas-phase products of incomplete conversion as these have the potential to adversely impact the application of the technology in occupied buildings. Thus, the study addresses the key research recommendations made by Tompkins et al. (2005a) as noted above.

METHODS

UVPCO Reactor and Flow System

The UVPCO reactor used for this study is based on a patented photocatalytic system developed by Titan Technologies (Sebastopol, CA). This system uses multiple honeycomb monoliths made of an optical polymer and coated with a thin semitransparent silane barrier coat followed by a thin semitransparent titanium dioxide (TiO₂) film serving as the photocatalyst. The monoliths are irradiated with 365-nm UV (UVA) lamps.

The device fabricated for the study contains four sections of removable monoliths. A schematic diagram of the device is shown in Figure 1. Each monolith has 10 cells per square centimeter and face dimensions of 30 by 30 cm (12 by 12 in). Monoliths with thickness of 1.25 and 2.5 cm (0.5 and 1.0 in) were used in three configurations. In two configurations, all four monoliths were either 1.25-cm or 2.5-cm thick (i.e., 5- or 10-cm total thickness). In the third configuration, two 2.5-cm thick monoliths were combined face-to-face in each section producing a total 20-cm monolith thickness. The monoliths are mounted in series, approximately 19 cm on

center, with their faces oriented transversely to the air flow path. Prior to first use, each set of monoliths was irradiated overnight under UVA lamps and then washed by immersion in 18.2 M Ω deionized water for 30 – 60 minutes. Excess water was removed by shaking, and then the monoliths were air dried and installed in the reactor. Monoliths were similarly treated when switching between VOC mixtures.

A total of nine UV lamps (Model F18T8/BL9/HO/BP, Voltarc Technologies, Inc., Waterbury, CT) are used. These 46-cm (18-in) long lamps produce about 2.8 Watts total UV with peak irradiance at 368 nm. Only about two-thirds of the lamp output is utilizable since the monolith face dimension is 30 cm. Device power consumption with all lamps on is 45 watts. The lamps are mounted transversely, 7.6 cm on center, in three banks of three lamps each. The banks are approximately centered between the monolith sections. The distance between a lamp surface and the face of a 2.5-cm thick monolith is about 7 cm. This lamp arrangement results in a reasonably uniform intensity distribution over the monolith faces.

Each monolith and lamp section is individually fabricated with sheet metal. These sections slip together in series and are fastened with sheet metal screws. All joints between sections are sealed with 5-cm wide aluminum duct tape. The inner duct dimensions of the reactor are 34 by 41 cm (13.5 by 16 in). The monoliths are centered within these dimensions and held in place by sheet metal webs and slip-tight frames.

Sheet metal pieces were fabricated to fit the inlet and outlet of the reactor. These pieces provided transitions from the rectangular reactor housing to 25-cm (10-in) diameter round sheet metal ducting. The upstream tapered transition (approximately 45-cm in length) was fitted with eight bored-through, 0.64-cm bulkhead unions (four each on two opposing sides of the transition) to provide ports for the collection of air samples. A temperature probe, a relative humidity (RH) probe, and a 0.32-cm OD tube for pressure monitoring additionally were installed in the center of the transition. Downstream, the transition went directly from the square reactor to a 60-cm long section of round ducting. This also was fitted with eight air-sampling ports arranged radially around the duct and with temperature and RH probes and pressure monitoring tubing.

A metal filter housing containing a pleated fabric air filter was installed at the inlet to the assembly. The filter element had a MERV 12 micro-particle performance rating and was built to

a custom size of 36 by 42 by 4.4 cm (Nordic Pure Air Filters, McKinney, TX). For the experiments conducted in the laboratory classroom (described below), there was no upstream ducting, and room air directly entered the filter. For the experiments in the environmental chamber, air entered the filter assembly through an approximate 7-m section of 20-cm (8-in) round corrugated aluminum ducting.

The 30-cm duct at the outlet of the assembly made an 180° turn and entered a venturi flow meter (Model NZP1031-10"-1-CF, Thermo Brandt Industries, Fuquay, NC) used for continuous monitoring of the air flow rate through the system. The outlet of the flow meter was connected to a duct blower (Model 207 INS, Delhi Industries, Inc., Delhi, Ontario, Canada) capable of providing 1,170 m³/h (690 cfm) air flow at 93 Pa (0.375-in of water) pressure drop. The duct blower exhausted through a rectangular mechanical damper used to establish the air flow rate through the system. The damper transitioned to a 30-cm (10-in) round corrugated aluminum ducting that exited directly to outdoors. All joints and seams throughout the entire system were carefully sealed with aluminum tape to minimize air leakage.

For these experiments, the UVPCO was operated at flow rate settings of approximately 175, 300, and 600 m³/h (100, 175, and 350 cfm). At these settings, the respective face velocities at the monoliths were 0.51, 0.89, and 1.78 m/s (100, 175, and 350 ft/min).

Monitoring Instrumentation

Temperatures, RH, and pressures were monitored continuously throughout each experiment with an Automated Performance Testing System (APTS) equipped with optional sensors and operating with data logging software (The Energy Conservatory, Minneapolis, MN). The APTS and the sensors were calibrated by the manufacturer immediately prior initiating the study. The monitored experimental parameters were: venturi flow meter reading; differential pressure between the duct and the room at the upstream and downstream locations; upstream, downstream, and room temperature; upstream, downstream, and room RH; and the ozone instrument signal in some experiments. The pressure measurements have a resolution of 0.1 Pa. The temperature sensor has an accuracy of $\pm 0.25^\circ$ C, and the RH sensor has an accuracy of $\pm 5\%$ RH. Data were recorded electronically at 30-sec intervals.

The analog voltage outputs of the 12 mass flow controllers used for collection of air samples (described below) were recorded with four-channel data loggers (Model U12-006, Onset Computer Corp., Bourne, MA). These data were recorded at 15-sec intervals.

Air Sampling

Air samples for the analysis of VOCs, low molecular weight aldehydes and ketones, and low molecular weight carboxylic acids were collected upstream and downstream of the UVPCO reactor section in each experiment. For each analyte type, there were three replicate samples collected simultaneously at both locations. The sampling media (described below) were connected to the bulkhead unions in the duct transition pieces. The VOC samplers were installed so the inlet ends extended approximately 4-cm into the air stream. Air flow rates through the three media types were regulated with electronic mass flow controllers (MFCs). There were six 0 – 500 standard cm³/min MFCs operated at approximately 100 cm³/min for the collection of VOC samples and six 0 – 2 standard L/min MFCs operated at approximately 1.5 L/min for the collection of aldehyde and acid samples. All MFCs were calibrated in the laboratory at standard conditions of 25° C and 101.3 kPa prior to initiating the study. Sample volumes were established by controlling the length of the sampling interval. The sampling interval for the aldehyde and acid samples was one hour. The sampling interval for the VOC samples was varied between 10 and 30 minutes depending upon the expected analyte concentrations; most VOC samples were collected over 30 minutes.

Air sampling for an experiment was initiated after the device had operated for at least one hour at the established conditions. Since the ventilation rates of the study environments were about four air changes per hour, or higher, inlet VOC concentrations were expected to be near steady-state conditions at this time. The sampling strategy was to first initiate the simultaneous collection of six VOC samples and six aldehyde samples. After the completion of aldehyde sampling, the simultaneous collection of six acid samples and a backup set of six VOC samples was initiated. Thus, the entire collection period extended over approximately two hours.

Air samples for the analysis VOCs were collected onto sorbent tubes (P/N CP-16251, Varian Inc., Walnut Creek, CA) packed with Tenax-TA™ with a 15-mm section of Carbosieve™ S-III 60/80 mesh (P/N 10184, Supelco Inc., Bellefonte, PA) substituted for the Tenax at the outlet end. Air samples for aldehydes were collected onto XpoSure Aldehyde Samplers (P/N

WAT047205, Waters Corp., Milford, MA). The sampling media for carboxylic acid samples were silica gel tubes treated with sodium hydroxide (P/N 22655, SKC-West, Inc., Fullerton, CA).

Chemical Analyses

VOC samples were analyzed by thermal desorption gas chromatography with mass selective detection and quantitation (TD-GC/MS) generally following U.S. EPA Method TO-1 (US EPA, 1984). Sample tubes were thermally desorbed and concentrated on a cryogenic inletting system (Model CP-4020 TCT; Varian, Inc.) fitted with a Tenax-packed trap (P/N CP-16425; Varian, Inc.). Tube desorption temperature was 235° C for 6.5 min. The cryogenic trap was held at -100° C and then heated to 235° C for injection. Compounds were resolved on a Hewlett-Packard (HP) Model 6890-II GC with a DB-1701 column (P/N 122-0733, Agilent Technologies) using the following cycle: 1° C for 1.33 min, 5° C/min to 225°C, and hold for 2 min. Compound mass was quantified with an HP Model 5973 MSD operated in electron ionization mode and scanned over m/z 30 – 350. Samples were analyzed on the day of collection or stored in a freezer for typically no more than one week before analysis. Most analytes were quantified using multi-point calibration curves developed from pure compounds (Aldrich, Milwaukee, WI). Quantitation was referenced to an internal standard of 1-bromo-4-fluorobenzene. Analytes (related mixtures of hydrocarbons) for which standards could not be obtained were identified using spectral libraries and quantified based on their total-ion-current (TIC) response, using the TIC current response of toluene as the reference.

Aldehyde air samples were analyzed for formaldehyde, acetaldehyde and 2-propanone (acetone) following ASTM Standard Method D 5197-97 (ASTM, 1997). Each sampling cartridge was extracted into 2 mL of acetonitrile. Extracts were analyzed by high-performance liquid chromatography (HPLC). The instrument was equipped with a diode array detector operated at a wavelength of 365 nm. Compounds were resolved on a Symmetry C₁₈, 2.1- by 150-mm column (P/N WAT056975, Waters Corp.). Analytes were quantified from multi-point calibrations of external standard mixtures.

The carboxylic air samples were analyzed for formic and acetic acids by ion chromatography following the method described in the manufacturer's product manual for the

analytical column (Dionex, 2002). Each sodium hydroxide coated cartridge was eluted with 18.2 MΩ deionized water into a 2-mL volumetric vial. These extracts were analyzed on a DX-120 ion chromatograph equipped with an AS40 automated sampler (Dionex Corp.). The compounds were resolved on an Ionpac® AS4A-SC analytical column, 4 by 250 mm (P/N 043174, Dionex Corp.) protected by an AG4A-SC guard column (P/N 043175, Dionex Corp.). The eluent was a water solution of 5 mM sodium tetraborate.

Additional Measurements

A recent study reported that hydrogen peroxide (H₂O₂) was generated by an experimental titania photocatalytic device (Kubo and Tatsuma, 2004). Thus, H₂O₂ in the exhaust of the study device was measured. The most sensitive analytical method involving chemical derivatization and analysis by HPLC with a fluorescence detector can achieve a detection limit of 1 ppb, or less. However, implementation of this method is difficult and was outside of the scope of the study. Instead, an instrument designed and used for industrial hygiene applications was selected. This instrument, the CMS Analyzer (P/N 6405300, Draeger Safety, Inc., Pittsburgh, PA), when equipped with a H₂O₂ specific chip (P/N 64006440, Draeger Safety, Inc.) achieves a sensitivity of 0.2 ppm. Measurements were obtained by placing the CMS Analyzer with the H₂O₂ chip directly in the exhaust duct downstream of the UVPCO while the device was operating in the classroom laboratory at both 170 and 580 m³/h.

The potential production or destruction of ozone in the UVPCO was measured during several experiments in the classroom laboratory. A calibrated ozone monitor (Model 1003AH, Dasibi Environmental Corp.) was alternately connected upstream and downstream of the reactor section. This instrument has a reported sensitivity of 1 ppb. Data were logged by the APTS.

Study Environments

The experiments with the UVPCO were conducted in two different environments. Experiments with the synthetic office VOC mixture (described below) were performed in relocatable school classroom sited at the LBNL campus and used as a laboratory for energy studies. This classroom laboratory was a doublewide manufactured structure with approximate interior dimensions of 7 by 12 m (23 by 39 ft) with a 2.6-m (8.5-ft) ceiling height. There were two exterior doors and no windows. The interior was bare with no partitions or built-in

cabinetry. The floor was carpeted, the walls were vinyl-covered fiberboard, and the ceiling was coated fiberglass acoustical panels. At the time of the experiments, the classroom contained tables, and some instrumentation and supplies used for other studies. The building was equipped with a packaged compressor-based HVAC system mounted on one exterior wall. For the experiments, the outside air (OA) dampers were fixed in the fully open position and the supply fan was operated continuously to deliver approximately 850 m³/h (500 cfm) of OA. The temperature of the classroom was regulated to near 23 ± 2° C. Humidity was unregulated. Both room temperature and humidity were monitored and logged. The UVPCO was sited directly in the space near one exterior doorway. The exhaust duct from the UVPCO was exited through a hole in a plywood panel fit to the doorway. The other door remained closed during an experiment.

The experiments with the building product mixture and the aldehyde mixture were conducted in a small laboratory containing a 20-m³ interior volume environmental chamber. The UVPCO was positioned outside the chamber. The chamber is constructed of low emitting materials and is lined with stainless steel. For these experiments, the air handling system supplying conditioned air to the chamber was disconnected and the exhaust was sealed. The 20-cm diameter inlet tubing for the UVPCO was run through the 30-cm diameter inlet opening to approximately the center of the chamber near the ceiling. With the UVPCO duct blower operating, supply air for the chamber was, thus, drawn from the laboratory through the unsealed portion of this opening. Exhaust air from the UVPCO was directed to outdoors through an opening in the laboratory wall. Ventilation air consisting of 100% OA is supplied to the laboratory at about 2,000 m³/h (1,200 cfm). An electric heater located in the chamber and regulated by a proportional controller maintained the temperature of the chamber near 23 ± 2° C.

Preparation and Introduction of VOC Mixtures

A synthetic mixture of VOCs frequently detected in office buildings was formulated based on data summarized in a review of VOC concentrations measured in North America since 1990 (Hodgson and Levin, 2003). The 27 compounds selected for the mixture represent broad ranges of chemical functionality and vapor pressure. The components of the mixture are listed in Table 1. In this table and in subsequent tables, target compounds are ordered by chemical class with oxygenated compounds listed at the top; and within each class, the compounds are listed in order

of decreasing volatility. In the data tables, some compounds are designated by the abbreviations shown in the second column of the mixture tables (Tables 1 and 2). The relative amounts of the individual compounds in the liquid mixture of office VOCs were based on their maximum reported mixing ratios or molar volume concentrations (parts per billion, ppb) in office buildings (ibid.). Three target levels were established at an approximate ratio of 1:3:10 (i.e., concentrations of the more abundant compounds were designed to be about one-half or one full order of magnitude higher than the concentrations of the least abundant compounds).

The liquid VOC mixture was introduced into the classroom laboratory at a controlled rate using a syringe pump (Model 975, Harvard Apparatus, Southnatic, MA). Either a 5-mL or a 10mL glass syringe was filled with the mixture. The syringe pump injection rate was set to produce the desired concentrations of VOCs in air. The syringe was connected to a tube that delivered the mixture to the surface of a heated glass dish in order to quickly evaporate the mixture. The air above the dish was locally ventilated with an oscillating fan operated on low setting.

A realistic mixture of VOCs emitted by products widely used to finish building interiors was generated by placing a number of these products directly into the 20-m³ chamber. The products consisted of gypsum board panels recently painted on both sides with a flat interior latex paint (10.2 m²), residential rebounded urethane carpet cushion (13.4 m²), three types of residential broadloom carpet (15.5 m² total area), a single hard-backed commercial carpet (3.4 m²), two types of residential sheet vinyl flooring (4.7 m² total area), mixed particle board panels (19 m² all exposed surfaces), a plywood panel (5.9 m² all exposed surfaces), a decorative plywood panel (5.9 m² all exposed surfaces), and a hardboard panel (5.9 m² all exposed surfaces). These products emitted a complex mixture of VOCs. The compounds quantified in the exhaust of the chamber are listed in Table 2. In some cases, compounds were aggregated into related, unspecified groups (e.g., C₁₁ alkyl substituted benzenes). The concentrations of these groups or mixtures were quantified using the summed total-ion current (TIC) responses of the individual chromatographic peaks with toluene as the standard. The combined masses of the listed compounds are estimated to account for 75 – 90% of the total mass of compounds emitted by the products. The chamber was continuously ventilated at a flow rate of about 175 m³/h or higher while the products were in the chamber.

The third mixture consisted of an aqueous solution of formaldehyde and acetaldehyde. A preservative-free formalin solution was prepared by refluxing approximately 1 g of paraformaldehyde (CAS # 30525-89-4) in 200 mL water for 1 hour. The concentration of formaldehyde in the solution was determined by spiking 1 μL of the resulting solution onto an aldehyde air sampling cartridge and analyzing it as described above. The measured concentration was 3.6 mg/mL. A 10-mL aliquot of this formalin solution was spiked with a measured micro-liter volume of pure acetaldehyde to produce a mixture of the two compounds. The mixture was injected into the 20- m^3 chamber by syringe pump as described above.

Experimental Matrix

Thirteen experiments were conducted using the three different mixtures of compounds (Table 3). Experiments 8 through 12 with the office VOC mixture were conducted in the classroom laboratory. Experiments 15 through 22 with the building product and aldehyde mixtures were conducted in the 20- m^3 chamber. Average device air flow rate, inlet gas temperature, and inlet relative humidity were calculated from data recorded at 30-second intervals for three periods respectively corresponding to the collection of VOC, aldehyde and carboxylic acid samples. The relative standard deviation of the flow rate measurements consistently was less than 2% over these intervals. The relative standard deviations for the temperature and humidity measurements consistently were less than 0.5%. Temperatures in the study spaces were regulated. These temperatures were near 23 – 24 $^{\circ}$ C and within the range of 22.7 to 24.4 $^{\circ}$ C. Humidities were unregulated and fell within the range of 44 to 57% RH.

Data Analysis

For each VOC, average concentrations in $\mu\text{g}/\text{m}^3$ were calculated from the individual sample masses and the respective sample volumes for all replicates ($n = 3$) collected at the upstream and downstream locations. These were converted to molar volume concentrations (i.e., mixing ratios) in ppb assuming standard conditions of 25 $^{\circ}\text{C}$ and 101.3 kPa (i.e., the calibration conditions for the sampling MFCs). Single-pass conversion efficiency, which represents the fraction of a compound removed from the air stream flowing through the reactor (i.e., the fraction reacted), was calculated for each analyte. This value was determined as one minus the quotient of the average outlet concentration and the average inlet concentration. For

reaction products, the fraction of compound produced was similarly calculated. The standard deviations of all calculated quantities were determined by error propagation.

The reaction rate of a compound was calculated by first converting the concentration of the compound to units of $\mu\text{moles}/\text{m}^3$ by multiplying the ppb concentration by the standard molar volume (i.e., 24.45 L). This value was then multiplied by the air flow rate through the reactor in m^3/h to yield a rate in μmoles compound per hour. Reaction rates in μmoles carbon per hour were calculated by multiplying the compound reaction rates by the number of carbon atoms in the individual compounds. This quantity allows direct comparison among compounds on a standard per carbon basis.

RESULTS

Effects of Monolith Thickness and Air Flow Rate

Five experiments were conducted in the classroom laboratory with the synthetic office VOC mixture. These experiments were designed to investigate the combined effects of monolith thickness and air flow rate through the UVPCO device on VOC reaction efficiency and rates.

Experiments 9, 10, and 12 were conducted at the low flow rate ($168 - 173 \text{ m}^3/\text{h}$) using combined monolith thicknesses of 5, 10, and 20 cm (2, 4, and 8 in). The upstream VOC mixing ratio, or concentration, in ppb for each of the compounds in the mixture, less acetone, are shown in Table 4 along with the fraction of each compound reacted (i.e., reaction efficiency). Acetic acid, a room air contaminant, also is included in the list of reactants. All values are presented as the mean plus or minus one standard deviation of the measurement except for acetic acid in Experiments 10 and 12 where only single acid samples were analyzed. The fraction reacted is not shown for a compound if the downstream measurement was not significantly lower than the upstream measurement at the 95% confidence level as determined by a one-tailed Student's *t* test. The fractions reacted for the 19 compounds with mostly significant upstream/downstream differences are plotted in Figure 2. In this and subsequent figures, uncertainties indicated by the error bars are two standard deviations of mean values.

The summed upstream air concentrations of spiked VOCs, including acetone, in the three experiments were 340 – 360 ppb. The supply rates of total compounds were 2,400 – 2,500

μmoles per hour. The upstream concentrations of individual VOCs also were similar across the three experiments.

For many of the 19 plotted VOCs, there was a trend of increasing reaction efficiency with increasing monolith thickness. In some cases, the overlapping error bars indicate that differences between successive increases in thickness likely were insignificant. For some compounds, such as isopropanol, phenol, and MTBE, the uncertainties were relatively large, potentially masking real differences among the treatments. For the five alcohols and the glycol ether 2-butoxyethanol (2-BE), reaction efficiencies even with the thinnest monoliths were around 0.7. With the thickest monoliths, the values for three of these compounds approached unity. Seven compounds consisting of all halogenated hydrocarbons and carbon disulfide were not significantly reacted in two or three of the experiments.

Experiments 8 and 11 were conducted at the high flow rate (602 and 589 m³/h) using combined monolith thicknesses of 10 and 20 cm (4 and 8 in). The upstream VOC mixing ratios and fractions of compounds reacted are shown in Table 5 for the spiked compounds, plus acetic acid and less acetone. The fractions reacted for the 12 compounds with significant upstream/downstream differences in both experiments are plotted in Figure 3. The summed upstream air concentrations of the spiked compounds in the two experiments were 290 – 310 ppb. The supply rates of total compounds were 7,100 – 7,500 μmoles per hour. The inlet concentrations of individual VOCs were similar between the two experiments. Also, the concentrations were similar to those in the low flow rate experiments.

When the high flow rate experiments are compared to their corresponding low flow rate experiments (i.e., for 10 and 20-cm monolith thicknesses), it is apparent that reaction efficiencies were consistently higher in the low flow rate experiments. This general relationship is expected due to the longer residence time of air within the reactor at 170 m³/h versus 600 m³/h.

For about one-half of the 12 plotted compounds, the highest reaction efficiencies were associated with the thickest monolith section. However, these differences likely are significant only for 2-ethyl-1-hexanol (ethylhexanol), 2-BE, and 1,2,4-trimethylbenzene (I,2,4-TMB). For ethylhexanol, phenol, and 2-BE, the fraction reacted was near 0.8 with the 20-cm monolith thickness. A number of compounds were not significantly reacted in one or both of the experiments. These compounds were ethanol, MTBE, 2-butanone, toluene, three alkane

hydrocarbons (n-nonane, n-decane, and n-undecane), all halogenated hydrocarbons, and carbon disulfide.

VOC reaction rates in $\mu\text{moles VOC per hour}$ and $\mu\text{moles carbon per hour}$ for Experiments 9, 10, and 12 are presented in Table 6, and reaction rates for Experiments 8 and 11 are presented in Table 7. The values are means plus or minus one standard deviation. Values are not shown for a compound if the downstream concentration was not significantly lower than the upstream concentration. Mean reaction rates in $\mu\text{moles carbon per hour}$ are plotted in Figure 4 for the 19 compounds in Experiments 9, 10, and 12 with significant concentration differences. In Figure 5, reaction rates are plotted for the 12 compounds in Experiments 8 and 11 with significant differences.

A comparison of Figures 4 and 5 reveals that the overall reaction rates for some compounds were similar at the two flow rate conditions. Compounds with generally similar rates include isopropanol, 1-butanol, hexanal, m-xylene, 1,2,4-TMB, and decamethylcyclotrisiloxane (D5). Ethylhexanol, phenol 2-BE, and d-limonene (limonene) had higher reaction rates at the high flow rate, while n-dodecane had lower reaction rates at the high flow rate. At both low and high flow rates, VOC reaction rates generally exhibit similar responses with respect to monolith thickness as demonstrated by the corresponding reaction efficiencies. The indicated uncertainties in the measurements suggest that a number of these differences are not significant.

The experiments with the synthetic office VOC mixture resulted in the production of formaldehyde, acetaldehyde, and acetone, which was a component of the spiked mixture (Tables 8 and 9). Acetic acid, as discussed above, was reacted, and formic acid concentrations in both upstream and downstream samples mostly were below the lower limit of quantitation of approximately 3 ppb. For Experiments 9, 10, and 12 conducted at the low flow rate, there was either only a small or insignificant increase in formaldehyde concentration in air exiting the reactor; the increases in acetaldehyde and acetone concentrations were in the range of 20 to 25 ppb (Table 8). For the high flow rate experiments (Table 9), there were larger increases in the downstream formaldehyde concentrations and smaller increases in the downstream concentrations of acetaldehyde and acetone relative to corresponding the low flow rate experiments.

The production rates of formaldehyde, acetaldehyde, and acetone in these experiments are shown in Tables 10 and 11. Formaldehyde production rates were substantially higher at the high flow rate. For both acetaldehyde and acetone, production rates were similar in all experiments with no obvious trends related to monolith thickness or flow rate.

Total-ion-current chromatograms of upstream and downstream VOC samples for the synthetic office VOC mixture were compared for each experiment to determine if intermediate reaction products within the volatile range were present downstream. Upstream and downstream chromatograms from Experiment 10 conducted at the low flow rate are shown in Figure 6. The comparison indicated that a small amount of butyl formate (CAS # 592-84-7) was formed.

Effect of UV Power

Four experiments were conducted in the 20-m³ environmental chamber with the building product mixture of VOCs. These experiments were designed to investigate the effect of UV power, manipulated by changing the number of lamps, on VOC conversion efficiencies and reaction rates.

For these experiments, the UVPCO device was configured with four 1-in monoliths. For Experiments 15 and 16, the standard lamp configuration of three lamps per bank (nine lamps total) was used. For Experiment 17, the middle lamp in each bank was removed (six lamps total). For Experiment 18, the device was operated with only the middle lamp in each bank (three lamps total). In Experiments 15, 17, and 18, the device was operated at the low flow rate (168 – 176 m³/h). The maximum flow rate (303 m³/h) obtainable with the duct configuration for these experiments was used in Experiment 16.

The upstream VOC concentrations and the fractions of these VOCs reacted are shown in Table 12. The summed upstream concentrations of the 19 target compounds and mixtures measured by TD-GC/MS, plus acetone, were 220 ppb for Experiment 16, 290 ppb for Experiments 15 and 17, and 250 ppb for Experiment 18. The respective supply rates of target VOCs to the reactor were 2,800, 2,000 – 2,100, and 1,740 μmoles/h. The concentrations of the individual VOCs were similar in Experiments 15, 17, and 18 conducted at 168 – 176 m³/h; concentrations were mostly lower in Experiment 16 in which the chamber was ventilated at a higher air flow rate. The results show that acetic acid and hexanal were produced in Experiment

18 with three lamps. In two or more experiments, downstream/upstream concentration differences were insignificant for hexanal, toluene, C₁₁ alkane hydrocarbons, and n-undecane.

The fractions reacted for the 15 compounds and mixtures with significant upstream/downstream differences are plotted in Figure 7. The reaction efficiencies of the plotted alcohols and glycol ethers were near 0.8 in all low flow rate experiments. For some VOCs, the reaction efficiencies were lowest for Experiment 18 with three lamps. These compounds were 2,2,4-trimethyl-1,3-pentanediol monoisobutyrate (TMPD-MIB), aromatic hydrocarbons from 1,2,4-TMB through the C₁₂ alkyl substituted benzenes, and three normal alkane hydrocarbons. Differences between Experiments 17 and 15 with six and nine lamps, respectively, were small and likely insignificant. Generally, the comparison of results for Experiments 15 and 16 respectively conducted at the low and high flow rates with nine lamps, shows that reaction efficiencies were lower in Experiment 16; but, often the uncertainties overlapped indicating insignificant differences.

VOC reaction rates in $\mu\text{moles VOC per hour}$ and $\mu\text{moles carbon per hour}$ for the four experiments are presented in Table 13. Mean reaction rates in $\mu\text{moles carbon per hour}$ are plotted in Figure 8 for the 15 compounds and mixtures with significant concentration differences. Reaction rates were mostly lowest in Experiment 18 with three lamps. The relatively low uncertainties suggest the differences often were significant. The differences between Experiments 17 and 15 with six and nine lamps, respectively, were small and likely insignificant except for 2-(2-butoxyethoxy) ethanol (DEGBE) and TMPD-MIB. The differences between Experiments 15 and 16, respectively conducted with nine lamps at the low and high ventilation rate, were small and likely insignificant except for ethylene glycol, a compound that is difficult to measure accurately and precisely.

The experiments with the building product mixture of VOCs resulted in the production of formaldehyde, acetaldehyde, and acetone (Tables 14 and 15). Acetic acid was produced in the two experiments with nine lamps. Formic acid concentrations in both upstream and downstream samples mostly were below the lower limit of quantitation. The downstream increases in formaldehyde concentrations were highest for Experiments 17 and 18 with the reduced numbers of lamps; for acetaldehyde and acetone there were no obvious relationships between the downstream increases in concentration and the numbers of lamps (Table 14). Increases in

downstream concentrations were generally lowest for Experiment 16 conducted at the higher flow rate and all nine lamps. Considering the uncertainties in the measurements, differences in compound production rates among the four experiments were small for formaldehyde, acetaldehyde, acetone, and acetic acid (Tables 13 and 15).

Total-ion-current chromatograms of upstream and downstream VOC samples were compared for each experiment to determine if intermediate reaction products within the volatile range were present downstream. Upstream and downstream chromatograms from Experiment 15 conducted with nine lamps at the low flow rate are shown in Figure 9. The comparison indicated that no reaction products were apparent within this range other than acetone.

Effect of Aldehyde Concentration

Four experiments were conducted in the 20-m³ environmental chamber with the aldehyde mixture. These experiments were designed to investigate the effect of concentration on aldehyde reaction efficiencies and rates. For these experiments, the UVPCO device was configured with four 1-in monoliths and nine lamps and was operated at 169 and 280–299 m³/h. The upstream formaldehyde concentrations ranged from 24 to 88 µg/m³; and the upstream acetaldehyde concentrations ranged from 9 to 23 µg/m³.

The upstream and downstream concentrations of formaldehyde, acetaldehyde, and acetone are shown in Table 16. As for the experiments with the building product mixture, ventilation air for the chamber was drawn from the laboratory. Upstream and downstream concentrations of total VOCs were quantified from the summed total-ion-current (TIC) responses of the individual chromatographic peaks with toluene as the standard. The upstream total VOC concentrations ranged from 44 to 70 µg/m³, and the downstream concentrations consistently were about 20 µg/m³ lower. This indicated reaction of background compounds may have resulted in some underdetermined production of formaldehyde, acetaldehyde, and acetone. Formaldehyde net reaction efficiencies are plotted in Figure 10. Conversion was highest and approached unity in Experiment 19 conducted at the low flow rate. In Experiment 20 with similar starting conditions but a higher air flow rate, the reaction efficiency was lower; although, the difference in efficiency relative to Experiment 19 likely was insignificant. The reaction efficiency in Experiment 22 with an 88 ppb upstream concentration was similar. The result for Experiment 21 appears to be anomalously low relative to the other high flow rate experiments; however, there is

no obvious explanation or reason to exclude this result. There was significant reaction of acetaldehyde only in Experiment 19 at the low flow rate. Acetone was the only VOC produced in these experiments (Table 16). This may have resulted from the reaction of unspecified VOCs as noted above. Upstream and downstream acetic acid concentrations generally were similar and less than 5 ppb in all experiments. Formic acid concentrations were below the lower limit of quantitation.

The reaction rates of formaldehyde and acetaldehyde in Experiments 19 – 22 are shown in Table 17. Formaldehyde reaction rates are plotted in Figure 11. Formaldehyde results for Experiments 19 and 20 with similar inlet concentrations are indistinguishable. Reaction rates are substantially higher in Experiment 22 with the 88 ppb upstream concentration.

Relative Reaction Efficiencies

The reaction efficiency data from low flow rate Experiments 10, 15, and 19 conducted with the synthetic office VOC mixture, the building product mixture, and the aldehyde mixture, respectively, were aggregated to evaluate the relative reaction efficiencies of all study compounds. In total, data were generated for 42 individual compounds or closely related groups of VOCs, six of which appeared in both mixtures. The compounds are listed in descending reaction efficiency order in Table 18. The exact order of the compounds is not highly relevant as there are considerable uncertainties in the measurements. Some of compounds were either insignificantly reacted or had reaction efficiencies of less than 10%. These included many of the halogenated hydrocarbons, the more volatile alkane hydrocarbons, toluene, 2-butanone, and carbon disulfide. Compounds with the highest reaction efficiencies (79 – 92%) included formaldehyde, many of the alcohols, and all of the glycol ethers. The most volatile alcohols, ethanol and isopropanol; the esters TMPD-MIB and TMPD-DIB; limonene; many of the less volatile aromatic hydrocarbons, and D5 siloxane, had somewhat lower reaction efficiencies. There were substantial differences between the results obtained with the office VOC and building products mixtures for four of the six compounds appearing in both mixtures. In all cases, the highest reaction efficiencies occurred in Experiment 10 with the office VOC mixture. For example, 1,2,4-TMB and hexanal were efficiently consumed (70%) in Experiment 10 but had reaction efficiencies of 14% and <10%, respectively, in Experiment 15. The individual upstream concentrations of these compounds were about 2 ppb in Experiment 10 and about 1

ppb in Experiment 15. N-Undecane and n-dodecane also exhibited a trend of higher reaction efficiencies in the office VOC mixture versus the building product mixture.

Pressure Drop and Additional Measurements

Duct pressure relative to the room was monitored upstream and downstream of the reactor section during all experiments except Experiments 21 and 22. Pressure drop across the reactor was determined as the difference between the upstream and downstream measurements. In all experiments conducted at low flow rate (168 – 176 m³/h) with four 2.5-cm monoliths, the pressure drop was 5 – 6 Pa. The pressure drop at intermediate flow rate (294 and 303 m³/h) was 12 – 13 Pa. In Experiment 11 at high flow rate (589 m³/h), the pressure drop was 25 Pa. In Experiment 8 at high flow rate (602 m³/h) with eight 2.5-cm monoliths, the pressure drop was 44 Pa. These pressure drops are small relative to total pressure drops in supply airstreams of HVAC systems, which often exceed 500 Pa. In Figure 12, pressure drop is plotted versus air velocity through the reactor equipped with four 2.5-cm monoliths. The data fit a least-squares linear regression with a forced zero intercept ($r^2 = 0.96$).

During experiments with the synthetic office VOC mixture, measurements of hydrogen peroxide (H₂O₂) were attempted in the UVPCO exhaust just downstream of the venturi flow meter at both the low and high flow rate and with and without injection of the VOC mixture. In no case was H₂O₂ detected above the reported 0.2 ppm sensitivity limit of the CMS Analyzer. Ozone was alternately monitored upstream and downstream of the reactor section in Experiments 9 – 11. In the low flow rate experiments, the upstream ozone concentrations were 17±1 ppb and the downstream concentrations were 12±1 ppb (Experiment 9) and 14±1 ppb (Experiment 10). In the high flow rate experiment (Experiment 11), the upstream ozone concentration was 14±2 ppb and the downstream concentration was 12±1 ppb. These results indicate a small amount of ozone destruction in the UVPCO.

DISCUSSION

In the following discussion, some of our analyses compare the observed performance of the UVPCO device with its predicted performance. These predictions were made using a photocatalytic monolith simulation, which incorporates sub models for light intensity distribution, mass transport and reaction kinetics. The details of the simulation software are

proprietary to Titan Technologies. Rate constants for many of the compounds used in the simulation were based on an aggregate analysis of the data set generated by these experiments.

Effects of Monolith Thickness

Increasing the thickness of the monolith will result in a longer gas residence time within the monolith volume and in a higher specific surface area of catalyst surface exposed to the gas stream. As this particular UVPCO device employs a semitransparent monolith design, an increase in monolith thickness is expected to result in general increases in both reaction efficiencies and absolute reaction rates for VOCs amenable to destruction by photocatalysis. However, the useful depth of a semitransparent monolith is dictated by its performance characteristics.

UV light is absorbed by the photocatalyst as it passes through the monolith resulting in substantially lower UV flux within the core of the monolith than at its illuminated face. Figure 13 shows the predicted relative UV flux as a function of depth for a representative slice of a 1-in thick monolith irradiated on one face with three lamps. This prediction was made using a numerical light distribution model of the lamp/monolith system employed here. There is an expected overall 100-fold decrease in UV flux with depth. This reduced UV flux within the core of the monolith results in lower VOC decomposition rates since these rates are dependent upon flux. However, the reaction order in light intensity is reported to be about 0.5 at the light intensities in question (e.g., Obee, 1996). Therefore, a reasonable level of photocatalytic activity is retained within the monolith. For example, 10% of the photocatalytic activity is expected to be retained at the point within the monolith where the light intensity is decreased by a factor of 100 relative to the face.

The data for VOCs with significantly lower downstream concentrations in Experiments 9, 10, and 12 generally trend in the predicted direction, i.e., reaction efficiencies and rates increased with monolith thickness. However, the analysis of this relationship is confounded for many compounds by their high reaction efficiencies and by the high measurement uncertainties relative to the small, observed differences. In addition, differences in the physical properties of the individual monolith panels and the physical alignment of channels when two 1-in panels are stacked face-to-face likely will affect the system's efficiency and may have contributed to some of the observed variation in results among the experimental conditions.

Nine of the VOCs plotted in Figure 2 achieved a reaction efficiency of about 90%. This was accomplished with four monoliths and three banks of lights (i.e., six irradiated monolith faces). Thus, the reaction efficiency associated with each face is estimated to be about 30%. For the middle two monoliths, which are irradiated on both faces, the reaction efficiency may be as high as 50%. Figure 14 plots the predicted reaction efficiency in percent as a function of relative photocatalytic activity for a 1-in monolith irradiated on one face with three lamps and operated at 175 m³/h. As shown, the predicted reaction efficiency approaches 28% at high photocatalytic activity. This is in agreement with the data for the nine most reactive VOCs in Experiment 9, which was operated with eight 1-in monoliths arranged in four sets. For these compounds, reaction efficiency is not so much a measure of photocatalytic activity but more correctly a measure of the mass transport limitations of the system.

Table 19 compares the measured and predicted effect of monolith thickness on reaction efficiency for phenol and limonene, two of the highly reactive VOCs that commonly are found in buildings. Within the uncertainties of the measurements, there is excellent agreement between observed and theoretical results.

Effects of Air Flow Rate

Increasing the air flow rate through the UVPCO device is expected to decrease reaction efficiency since the lower residence time of the air in the monoliths allows less time for compounds to adsorb to the catalyst surface. However, this effect is offset because increased gas velocity will improve the mass transfer of VOCs to the catalyst surface. It also is important to note that increasing gas velocity will not result in a proportional decrease in reaction efficiency even in the absence of mass transfer effects since the reaction kinetics are proportional to the concentration of a reactant. Another complicating factor is that performance at the leading edge of the system is predicted to decrease at higher gas velocities. In this case, the contaminants are presumed to pass on to the catalyst surface later in the gas flow path, increasing the reaction rates in that area.

Although the reaction kinetics parameter is somewhat more complicated than first order, the relationship between reaction efficiency and residence time is approximated reasonably well by an exponential function.

$$\text{residence time} \propto -\ln(1 - \text{reaction efficiency})$$

For example, if the reaction efficiency is 90% at a particular residence time, halving the residence time by doubling the gas velocity will yield 68% reaction efficiency. If another residence time yields 40% reaction efficiency, doubling the gas velocity will reduce the reaction efficiency to 22%. These examples illustrate that the predicted effect is highly nonlinear for compounds with high reaction efficiencies and nearly proportional for compounds with lower reaction efficiencies. If there is mass transport resistance, then increasing the velocity will increase mass transport and increase the absolute reaction rate at all points in the monolith. Thus, for a highly reactive VOC limited by mass transport, the reaction efficiency still decreases with increased velocity, but the effect is attenuated by the increased absolute reaction rate.

The effect of increasing the air flow rate through the UVPCO device was examined in paired Experiments 8 and 9, 10 and 11, 15 and 16, and 19 and 20. For the first two pairs, the high flow rate was a factor of 3.4 – 3.5 higher than the low flow rate; and for the latter two pairs the factor was 1.7. Overall, increased gas velocity caused a decrease in the reaction efficiency for nearly all reactive VOCs as expected. For some VOCs (i.e., MIBK, m-xylene, and C₁₀–C₁₂ normal alkanes), the decrease was approximately proportional to the low rate increase or was higher than expected. For all of the more reactive VOCs, the decrease in performance was less than predicted, based solely on residence time. As one example, the reaction efficiency for phenol of 87% in Experiment 15 at 176 m³/h is expected to decrease to 69% when the flow rate is increased to 303 m³/h in Experiment 16. The actual decrease in reaction efficiency to 76% was less, presumably due to an increase in mass transfer at the higher velocity. For the same experiment pair, the reaction efficiency for the group of C₁₀ alkylbenzenes decreased from 56% to 41% in near agreement with the predicted decrease to 38%. The implication is that mass transport resistance is not large in this latter case, so an effect due to improved mass transfer is not apparent.

Correcting for the effect of mass transfer, measured reaction efficiencies as a function of air flow rate are in agreement with predicted values for most compounds with significant reactivity. This result suggests that the gas velocity in the UVPCO device should be kept above the values used in the low flow rate experiments to most effectively utilize the available monolith surface area and the UV light flux. For a given gas flow rate, a UVPCO device with a small cross

sectional area operating at high velocity may exhibit only a modest decrease in performance relative to a larger device placed within the same HVAC system. In one possible configuration, two small cross section systems in series may give improved performance compared to a larger cross section, single system of the same total monolith volume. In practice, the feasibility of this and other alternate configurations depends, in part, on the overall pressure drop of the system.

Effect of UV Power

Photocatalytic decomposition reactions are driven by photon absorption. A higher UV flux will lead to more hydroxyl radicals and higher reaction efficiency. However, most of the electron-hole pairs that are formed in the semiconductor will recombine. The bimolecular nature of the recombination reaction leads to a reaction order in light intensity of approximately 0.5. Thus, there is a diminishing return in performance as more UV power is added to the system. All else being equal, doubling the UV power will increase performance by about 40% while tripling the UV power will yield only a 70% improvement in performance. In practice, the gain in performance is expected to be less because not all of the photons from a lamp reach the monolith surface. For example, adding additional lamps generally results in lamp surfaces being placed closer to duct walls, which increases the amount of lost light.

The effect of UV power on performance of the UVPCO device was examined in Experiments 15, 17, and 18 conducted at $\sim 168 \text{ m}^3/\text{h}$ with the building product mixture of VOCs. For many of the VOCs in this mixture, the observed effects of UV power notably were small. A possible explanation for compounds with relatively high reaction efficiencies is that performance is primarily controlled by mass transport to the catalyst surface as discussed above. Thus, even with only one lamp in each section, there presumably is sufficient photocatalytic activity to decompose most of the mass of reactive VOCs that reach the catalyst surface. Increasing UV power by adding lamps to each section is expected to have only small effects on observed efficiencies for these VOCs.

An effect of increased lamp power, however, is expected for compounds that are not as easily decomposed. This trend was observed for many, although not all, compounds with reaction efficiencies $< 60\%$. For example, as shown in Table 20, the measured effect of increased UV intensity agrees well with predicted values for the group of C_{10} alkylbenzenes. Increasing the number of lamps from three to nine increased the reaction efficiency for the C_{10}

alkylbenzenes by about 87%, which is in reasonable agreement, considering uncertainties, with the 70% increase predicted by the simulation model.

Because of the high reaction efficiencies of many of the compounds in the challenge mixture, this series of experiments turned out to be of limited value in demonstrating the effect of changes in UV power on performance. However, there were enough compounds with lower reaction efficiencies to show that UV power does, indeed, affect performance.

Effect of Aldehyde Concentration

The results of Experiments 19 – 22 show that formaldehyde was easily decomposed by the UVPCO device. In fact, formaldehyde decomposition likely occurred at near the mass transport limited rate. Experiments 19 and 20 conducted at two air flow rates (169 and 294 m³/h, respectively) with low upstream concentrations of formaldehyde (24 and 30 ppb, respectively) indicate that the difference in reactivity was less than predicted due solely to the difference in flow rate. Ignoring the possibly anomalous Experiment 21, a change in formaldehyde concentration from 24 to 88 ppb did not have an effect on conversion efficiency. However, the overall rates are higher than predicted based on previous unreported experiments performed by Titan Technologies at low part-per-million formaldehyde concentrations. At 1 ppm formaldehyde, the expected reaction efficiencies at the 169 and 294 m³/h air flow rates are 62% and 47%, respectively. These rates compare to the respective observed efficiencies of 92% and 67%. The relatively large differences illustrate that extrapolation of data collected at high concentration may under-predict performance at low, realistic building concentrations. Increased competition for active sites on the catalyst surface at higher concentration provides a possible explanation.

Reaction Products

Formaldehyde, acetaldehyde, and acetone were produced as reaction products in these experiments. With the exception of acetic acid in the experiment with three lamps, no other significant byproducts were identified by the sampling and analytical methods employed by the study. A comparison across all experiments of the production rates of these three carbonyl compounds in $\mu\text{moles carbon per hour}$ ($\mu\text{moles C/h}$) to the decomposition rates in $\mu\text{moles C/h}$ of all VOCs with significantly lower downstream concentrations, shows that 14 – 26% (mean \pm one

standard deviation = $22 \pm 4\%$, $n = 9$) of the carbon introduced into the device was converted to these reaction products instead of being completely oxidized to carbon dioxide. Acetone, a chemical with relatively low toxicity, comprised a substantial fraction of the products formed (0.62 ± 0.05 , $n = 9$). In experiments with the synthetic office VOC mixture, acetaldehyde accounted for most of the remainder, while in the experiments with the building product mixture both formaldehyde and acetaldehyde were produced with formaldehyde predominating. Since formaldehyde also was efficiently converted by the device, the observed formaldehyde production rates are net values.

The formation of products of incomplete oxidation by the UVPCO device presumably is related to the VOC composition of the air entering the device. The acetaldehyde produced in the experiments with the synthetic office VOC mixture may have derived directly from the oxidation of ethanol. For the four experiments with significant reaction of ethanol, the ratio of acetaldehyde production in $\mu\text{moles/h}$ to ethanol destruction in $\mu\text{moles/h}$ ranged between 0.56 and 0.89. Notably, formaldehyde production in the experiments with the synthetic office VOC mixture was low. The oxidation of ethylene glycol is a possible direct source of formaldehyde production in the experiments with the building products mixture. In Experiments 15 and 16 with all nine lamps, the ratio of formaldehyde net production in $\mu\text{moles/h}$ to ethylene glycol destruction in $\mu\text{moles/h}$ was 0.37 and 0.28, respectively. This ratio increased with the removal of lamps to 0.58 and 0.79 in Experiments 17 and 18, respectively.

The design of a UVPCO device for commercial use in occupied buildings must minimize the production unwanted byproducts. In particular, there is concern about introducing sources into buildings that can result in elevated concentrations of formaldehyde and acetaldehyde. These two chemicals are categorized as carcinogens on the State of California Safe Drinking Water and Toxic Enforcement Act of 1986 (Proposition 65) list of toxicants (OEHHA, 2005a). The World Health organization recognizes formaldehyde as a carcinogen (IRAC, 2004). In addition, noncancer guideline concentrations for determining the acceptability of exposures to formaldehyde and acetaldehyde among the general population including sensitive individuals (OEHHA, 2005b) are quite low, often lying below concentrations encountered in buildings. For formaldehyde, the one-hour acute Reference Exposure Level (REL) is 74 ppb, and the long-term (i.e., ten years or more) chronic REL is only 2.4 ppb (ibid.). The chronic REL for acetaldehyde is 5 ppb (ibid.). The California Air Resources Board's recommended guideline for formaldehyde

concentrations in buildings is 27 ppb, a value derived from the acute REL (CARB, 2004). Another concern not addressed in this study is the odor acceptability of UVPCO treated air due to the potential formation of products not detected by the employed sampling and analytical techniques.

SUMMARY AND RECOMMENDATIONS

The UVPCO device has high reaction efficiencies for VOCs commonly encountered in indoor environments including many alcohols, glycol ethers, formaldehyde, hexanal, d-limonene, higher molecular weight alkyl substituted benzenes, and decamethylcyclopentasiloxane. In the lower flow rate experiments, mass transfer effects likely limited the performance of the device for these highly reactive compounds. This finding along with the results from a limited number of experiments conducted at higher flow rates, indicate that the device is capable of achieving good conversion for these compounds at flow rates comparable to flow rates in HVAC systems operating in large buildings. The experiments also provided information on the effects of monolith thickness and UV power or light intensity. The results of the series of UV power experiments are particularly notable as they suggest the device is highly efficient in its use of light. A portion of the carbon that is reacted in the UVPCO ends up as intermediate byproducts consisting of acetone, formaldehyde, and acetaldehyde. The production of formaldehyde and acetaldehyde, which are potent toxicants, are of concern with respect to the use of an air cleaning technology in occupied environments. The results suggest that the formation of these two compounds is highly dependent upon the composition of the mixture of VOCs entering the device. This complicates a general assessment of the potential adverse impact of the technology on indoor air quality. Another potential limitation with respect to indoor applications is the selective nature of the reactions in which some classes of VOCs are not significantly oxidized. Despite these concerns, this UVPCO technology has high reaction efficiencies for a number of important classes of VOCs and has the potential to operate with high energy efficiency. Thus, further study and development of the technology seems warranted. The following recommendations provide an outline of near-term research to support this development.

- Design and conduct a series of experiments to further evaluate the effect of UV power on the performance of the UVPCO device. Based on the results of these experiments, optimize the design of the reactor to achieve the most cost effective destruction of VOCs.

- Conduct experiments in which the UVPCO device is challenged with single compounds or simple mixtures of compounds representative of VOCs in indoor air to determine which compounds and chemical classes lead to the highest net production of formaldehyde and acetaldehyde. Evaluate by laboratory experiments and modeling the likely effects of the UVPCO on indoor air concentrations of formaldehyde and acetaldehyde for various scenarios simulating how such a device might be installed in a building's supply air stream. Consider non-steady state conditions such as morning HVAC startup and the response of the device to episodic use of products that employ alcohols and glycol ethers as solvents. Evaluate the performance of the UVPCO in a large-scale chamber with recirculated air and compare the results to model predictions. Develop and evaluate options for reducing the impact of UVPCO air cleaning on indoor air concentrations of formaldehyde and acetaldehyde.
- Operate the UVPCO in several types of buildings such as offices, retail stores, and schools with different sources and concentrations of VOCs. Configure the installation of the device so the treated air exhausts directly to outdoors without any circulation. Measure single-pass conversion efficiencies and the production of reaction byproducts at building relevant device flow rates. Compare these results to laboratory-generated data.
- Operate the UVPCO continuously over extended periods of at least several months in a laboratory environment or in a building. Determine conversion efficiencies as a function of time, possibly by periodically challenging the UVPCO with a defined VOC mixture under controlled conditions. If decreases in reactivity are observed, determine if simple washing of the monoliths in water as described here restores performance.
- Refine models for estimating the costs of installing and operating a commercial UVPCO device for the treatment of air in office buildings, retail buildings, and schools. Estimate overall energy savings for different scenarios in which UVPCO and advanced particle filtration are substituted for 50% OA supply in these building types.

ACKNOWLEDGEMENTS

This work was supported by the Assistant Secretary for Energy Efficiency and Renewable Energy, Building Technologies Program of the U.S. Department of Energy under contract

DE-AC02-05CH11231. The authors thank Terry Logee of DOE for program management, David Faulkner of LBNL for assistance with logistics and data reduction, and Tosh Hotchi and Ray Dod of LBNL for assistance with analytical chemistry. Steve Sitkiewitz and Gary Carmignani of Titan Technologies are acknowledged for many helpful discussions throughout the study and for their review of this report. Hugo Destailats of LBNL also is acknowledged for his review.

REFERENCES

- Alberici RM, Mendes MA, Jardim WF, and Eberlin MN (1998) Mass spectrometry on-line monitoring and MS2 product characterization of TiO₂/UV photocatalytic degradation of chlorinated volatile organic compounds. *J. American Soc. For Mass Spectrometry* 9(12):1321-1327.
- ASTM (1997) *Standard Test Method for Determination of Formaldehyde and Other Carbonyl Compounds in Air (Active Sampler Methodology)*. Method D 5197-97, American Society for Testing and Materials, West Conshohocken, PA.
- CARB (2004) *Indoor Air Quality Guideline No. 1. Formaldehyde in the Home*. California Air Resources Board. <http://www.arb.ca.gov/research/indoor/formaldGL08-04.pdf>.
- Chen W, Zhang JS, and Zhang Z (2005) Performance of air cleaners for removing multi-volatile organic compounds in indoor air. *ASHRAE Transactions* 112(1).
- Dionex (2002) *Product Manual IONPAC® AG4-SC Guard Column, IONPAC® AS4A-SC Analytical Column*, Document No. 034528, Revision 07. Dionex Corporation.
- Disdier J, Pichat P, and Mas D (2005) Measuring the effect of photocatalytic purifiers on indoor air hydrocarbons and carbonyl pollutants. *J. Air & Waste Manage. Assoc.* 55:88-96.
- Ginestet A, Pugnet D, Rowley J, Bull K, and Yeomans H (2005) Development of a new photocatalytic oxidation air filter for aircraft cabin. *Indoor Air* 15(5): 326-334.
- Henschel DB (1998) Cost analysis of activated carbon versus photocatalytic oxidation for removing organic compounds from air. *J. Air & Waste Manage. Assoc.* 48:985-994.
- Hodgson AT, and Levin H (2003) Volatile organic compounds in indoor air: A review of concentrations measured in North America since 1990. Lawrence Berkeley National Laboratory, Berkeley, CA, Report No. LBNL-51715.
- IARC (2004) IARC Monographs on the Evaluation of Carcinogenic Risks to Humans. Formaldehyde, 2-butoxyethanol and 1-tert-Butoxy-2-propanol (Vol. 88, 2-9 June 2004). International Agency for Research on Cancer. <http://www-cie.iarc.fr/htdocs/announcements/vol88.htm>.
- Jacoby WA, Nimios MR, Blake DM, Noble RD, and Koval CA (1994) Products, intermediates, mass balances, and reaction pathways for the oxidation of trichloroethylene in air via heterogeneous photocatalysis. *Environ. Sci. Technol.* 28(9):1661-1668.

- Khalifa, HE (2005) Effect of nonuniform UV irradiation on photocatalytic air purifier performance. *ASHRAE Transactions* 111(2).
- Kubo W, and Tatsuma T (2004) Detection of H₂O₂ from TiO₂ photocatalyst to air. *Analytical Sciences* 20:591-593.
- Obee TN (1996) Photooxidation of sub-parts-per-million toluene and formaldehyde levels on titania using a glass-plate reactor. *Environ. Sci. Technol.* 30(12):3578-3584.
- OEHHA (2005b) *Air Toxics Hot Spot Program*. California Office of Environmental Health Hazard Assessment. <http://www.oehha.ca.gov/air/hot-spots/index.html>.
- OEHHA (2005a) *Proposition 65, The Safe Drinking Water and Toxic Enforcement Act of 1986*. California Office of Environmental Health Hazard Assessment. <http://www.oehha.ca.gov/prop65.html>.
- Tompkins DT, Lawnicki BJ, Zeltner WA, and Anderson, MA (2005a) Evaluation of photocatalysis for gas-phase air cleaning – Part 1: Process, technical and sizing considerations. *ASHRAE Transactions* 111(2).
- Tompkins DT, Lawnicki BJ, Zeltner WA, and Anderson, MA (2005b) Evaluation of photocatalysis for gas-phase air cleaning – Part 2: Economics and utilization. *ASHRAE Transactions* 111(2).
- US EPA (1984) *Method TO-1, Revision 1.0: Method for the Determination of Volatile Organic Compounds in Ambient Air Using Tenax® Adsorption and Gas Chromatography/Mass Spectrometry (GC/MS)*. Center for Environmental Research Information, Office of Research and Development, United States Environmental Protection Agency.
- Zeltner WA, and Tompkins DT (2005) Shedding light on photocatalysis. *ASHRAE Transactions* 111(2).

Table 1. Components of synthetic office VOC mixture

Compound	Abbreviation	CAS #	Chemical Class	Formula Weight
Ethanol		6417-5	Alcohol	46.07
2-Propanol	Isopropanol	67-63-0	Alcohol	60.10
1-Butanol		71-36-3	Alcohol	74.12
2-Ethyl-1-hexanol	Ethylhexanol	104-76-7	Alcohol	130.23
Phenol		108-95-2	Alcohol	94.11
2-Butoxyethanol	2-BE	111-76-2	Glycol ether	118.18
<i>tert</i> -Butyl methyl ether	MTBE	1634-04-4	Ether	88.15
2-Propanone	Acetone	67-64-1	Ketone	58.08
2-Butanone		78-93-3	Ketone	72.11
4-Methyl-2-pentanone	MIBK	108-10-1	Ketone	100.16
Hexanal		66-25-1	Aldehyde	100.16
d-Limonene	Limonene	5989-27-5	Terpene HC	136.24
Toluene		108-88-3	Aromatic HC	92.14
m-Xylene		108-38-3	Aromatic HC	106.17
1,2,4-Trimethylbenzene	1,2,4-TMB	95-63-6	Aromatic HC	120.20
n-Nonane		111-84-2	Alkane HC	128.26
n-Decane		124-18-5	Alkane HC	142.29
n-Undecane		1120-21-4	Alkane HC	156.31
n-Dodecane		112-40-3	Alkane HC	170.34
Trichlorofluoromethane	R-11	75-69-4	Halo HC	137.37
Dichloromethane	DCM	75-09-2	Halo HC	84.93
1,1,1-Trichloroethane	1,1,1-TCA	71-55-6	Halo HC	133.41
Trichloroethene		79-01-6	Halo HC	131.39
Tetrachloroethene	PCE	127-18-4	Halo HC	165.83
1,2-Dichlorobenzene	1,2-DCB	95-50-1	Halo HC	147.00
Carbon disulfide	CS ₂	75-15-0	Sulfide	76.14
Decamethylcyclopentasiloxane	D5	541-02-6	Siloxane	370.78

Table 2. VOCs quantified in air exhaust of 20-m³ chamber loaded with combination of building products

Compound	Abbreviation	CAS #	Chemical Class	Formula Weight
Phenol		108-95-2	Alcohol	94.11
Butylated hydroxytoluene	BHT	128-37-0	Alcohol	220.36
Ethylene glycol		107-21-1	Glycol ether	62.07
2-(2-Butoxyethoxy) ethanol	DEGBE	112-34-5	Glycol ether	162.23
Acetic acid		64-19-7	Acid	60.05
2-Propanone	Acetone	67-64-1	Ketone	58.08
Formaldehyde		50-00-0	Aldehyde	30.03
Acetaldehyde		75-07-0	Aldehyde	44.05
Hexanal		66-25-1	Aldehyde	100.16
2,2,4-Trimethyl-1,3-pentanediol monoisobutyrate (2 isomers)	TMPD-MIB	25265-77-4	Ester	216.32
2,2,4-Trimethyl-1,3-pentanediol diisobutyrate	TMPD-DIB	6846-50-0	Ester	286.41
Toluene		108-88-3	Aromatic HC	92.14
1,2,4-Trimethylbenzene	1,2,4-TMB	95-63-6	Aromatic HC	120.20
C ₄ Alkylbenzenes* (mixture)			Aromatic HC	134.22
Naphthalene		91-20-3	Aromatic HC	128.17
C ₁₀ Alkylbenzenes* (mixture)			Aromatic HC	218.38
C ₁₁ Alkylbenzenes* (mixture)			Aromatic HC	232.41
C ₁₂ Alkylbenzenes* (mixture)			Aromatic HC	246.44
C ₁₁ Alkane HCs* (mixture)			Alkane HC	156.31
n-Undecane		1120-21-4	Alkane HC	156.31
n-Dodecane		112-40-3	Alkane HC	170.34
n-Tridecane		629-50-5	Alkane HC	184.37
n-Tetradecane		629-59-4	Alkane HC	198.40

*Quantified using GC/MS total-ion-current response with toluene as standard

Table 3. Experimental conditions for 13 experiments conducted with UVPCO challenged with three VOC mixtures. Mean values are shown for three time periods corresponding to the collection of VOC, aldehyde and carboxylic acid samples

Exp No	Date	Mixture ^a	Monolith Config ^b	<i>Air Flow Rate (m³/h)</i>			<i>Inlet Air Temperature (°C)</i>			<i>Inlet Relative Humidity (%)</i>		
				VOC	Ald	Acid	VOC	Ald	Acid	VOC	Ald	Acid
8	6/13/05	Office	8x2.5-cm	602	600	597	23.4	23.6	23.6	53	52	52
9	6/15/05	Office	8x2.5-in	173	174	174	24.0	24.2	23.9	46	45	44
10	6/17/05	Office	4x2.5-cm	175	175	174	23.3	23.6	24.4	48	48	45
11	6/20/05	Office	4x2.5-cm	589	588	587	23.1	23.5	23.1	50	50	51
12	6/22/05	Office	4x1.25-cm	168	167	167	24.4	24.0	23.7	50	52	53
15	8/02/05	Bld Prod	4x2.5-cm	176	175	177	22.7	22.7	22.7	56	56	57
16	8/02/05	Bld Prod	4x2.5-cm	303	304	304	23.0	23.2	23.6	56	56	55
17	8/03/05	Bld Prod	4x2.5-cm ^c	168	168	168	23.2	23.2	23.4	56	56	55
18	8/04/05	Bld Prod	4x2.5-cm ^d	168	168	168	23.2	23.2	23.2	56	57	57
19	8/18/05	Aldehyde	4x2.5-cm	169	169	169	24.0	23.8	24.0	51	51	51
20	8/19/05	Aldehyde	4x2.5-cm	294	294	294	22.8	22.9	22.9	54	54	53
21	8/23/05	Aldehyde	4x2.5-cm	300	299	297	23.4	23.5	23.9	53	53	52
22	8/24/05	Aldehyde	4x2.5-cm	280	280	283	23.5	23.5	24.1	50	50	50

- a. Office = synthetic office VOC mixture; Bld Prod = VOCs from building products; Aldehyde = formaldehyde and acetaldehyde mixture
- b. All experiments conducted with nine lamps unless otherwise indicated
- c. Six lamps (i.e., inner lamp in each of three banks removed)
- d. Three lamps (i.e., outer lamps in each of three banks removed)

Table 4. Upstream VOC mixing ratios (ppb) and fractions of VOCs reacted (mean \pm 1 std. deviation) in UVPCO challenged with synthetic office VOC mixture and operated at approximately 170 m³/h (100 cfm) with three monolith configurations

Compound	<i>Exp 12 Four 0.5-in Monoliths</i>		<i>Exp 10 Four 1-in Monoliths</i>		<i>Exp 9 Eight 1-in Monoliths</i>	
	Mix Ratio (ppb)	Fraction Reacted	Mix Ratio (ppb)	Fraction Reacted	Mix Ratio (ppb)	Fraction Reacted
Ethanol	55 \pm 2	0.68 \pm 0.06	50 \pm 4	0.53 \pm 0.11	55 \pm 1	0.70 \pm 0.03
MTBE	9.3 \pm 1.1	0.24 \pm 0.14	8.8 \pm 0.9	0.37 \pm 0.22	8.3 \pm 0.7	0.29 \pm 0.19
Isopropanol	38 \pm 3	0.75 \pm 0.12	34 \pm 4	0.67 \pm 0.14	37 \pm 2	0.85 \pm 0.07
1-Butanol	3.4 \pm 0.2	0.71 \pm 0.06	3.7 \pm 0.1	0.79 \pm 0.05	4.0 \pm 0.1	0.91 \pm 0.02
2-Butoxyethanol	7.3 \pm 0.1	0.72 \pm 0.03	7.5 \pm 0.1	0.85 \pm 0.02	7.8 \pm 0.2	0.98 \pm 0.03
2-Ethyl-1-hexanol	5.0 \pm 0.1	0.68 \pm 0.01	5.0 \pm 0.1	0.81 \pm 0.03	5.2 \pm 0.1	0.96 \pm 0.03
Phenol	2.2 \pm 0.3	0.77 \pm 0.15	1.91 \pm 0.10	0.85 \pm 0.07	2.1 \pm 0.1	0.95 \pm 0.02
Acetic acid	8.1	>0.63	7.9 \pm 1.9	>0.62	7.2 \pm 2.9	Ns*
2-Butanone	3.3 \pm 0.1	0.18 \pm 0.08	3.2 \pm 0.3	Ns	3.5 \pm 0.2	0.26 \pm 0.09
MIBK	7.8 \pm 0.5	0.42 \pm 0.07	8.0 \pm 0.1	0.46 \pm 0.05	8.0 \pm 0.2	0.62 \pm 0.04
Hexanal	2.0 \pm 0.1	0.61 \pm 0.09	2.2 \pm 0.1	0.70 \pm 0.05	2.2 \pm 0.1	0.86 \pm 0.05
d-Limonene	4.7 \pm 0.2	0.59 \pm 0.05	3.7 \pm 0.2	0.75 \pm 0.06	4.1 \pm 0.2	0.94 \pm 0.06
Toluene	25 \pm 1	Ns	26 \pm 1	0.05 \pm 0.04	25 \pm 1	0.08 \pm 0.03
m-Xylene	7.8 \pm 0.5	0.18 \pm 0.06	8.2 \pm 0.1	0.46 \pm 0.04	8.2 \pm 0.2	0.71 \pm 0.04
1,2,4-TMB	2.4 \pm 0.1	0.44 \pm 0.01	2.4 \pm 0.1	0.70 \pm 0.03	2.4 \pm 0.1	0.92 \pm 0.03
n-Nonane	5.4 \pm 0.2	Ns	5.6 \pm 0.1	0.07 \pm 0.03	5.6 \pm 0.1	0.12 \pm 0.05
n-Decane	5.0 \pm 0.1	0.12 \pm 0.02	5.0 \pm 0.1	0.14 \pm 0.03	5.1 \pm 0.1	0.23 \pm 0.05
n-Undecane	4.4 \pm 0.1	0.25 \pm 0.01	4.3 \pm 0.1	0.27 \pm 0.04	4.5 \pm 0.1	0.42 \pm 0.05
n-Dodecane	11.9 \pm 0.3	0.35 \pm 0.03	11.8 \pm 0.1	0.41 \pm 0.04	12.0 \pm 0.2	0.60 \pm 0.04

Table 4. Continued.

Compound	<i>Exp 12 Four 0.5-in Monoliths</i>		<i>Exp 10 Four 1-in Monoliths</i>		<i>Exp 9 Eight 1-in Monoliths</i>	
	Mix Ratio (ppb)	<i>Reacted or Produced</i>	Mix Ratio (ppb)	<i>Reacted or Produced</i>	Mix Ratio (ppb)	<i>Reacted or Produced</i>
R-11	7.1±1.1	<i>Ns</i>	6.3±0.2	<i>Ns</i>	6.2±0.5	<i>0.16±0.12</i>
Dichloromethane	31±3	<i>Ns</i>	34±6	<i>Ns</i>	30±1	<i>Ns</i>
1,1,1-TCA	18.0±1.7	<i>Ns</i>	15.9±2.2	<i>Ns</i>	14.0±0.9	<i>Ns</i>
Trichloroethene	2.2±0.1	<i>Ns</i>	2.1±0.1	<i>Ns</i>	2.2±0.1	<i>Ns</i>
PCE	5.1±0.4	<i>Ns</i>	5.2±0.1	<i>Ns</i>	5.2±0.1	<i>Ns</i>
1,2-DCB	1.56±0.02	<i>Ns</i>	1.57±0.02	<i>0.04±0.02</i>	1.59±0.04	<i>Ns</i>
Carbon disulfide	3.7±0.3	<i>0.20±0.15</i>	3.4±0.4	<i>Ns</i>	3.4±0.1	<i>Ns</i>
D5	1.78±0.13	<i>0.47±0.08</i>	1.86±0.03	<i>0.64±0.03</i>	1.89±0.05	<i>0.86±0.03</i>

*Ns = Difference between upstream and downstream VOC concentration not significant at 95% confidence level by 1-tailed Student's t test

Table 5. Upstream VOC mixing ratios (ppb) and fractions of VOCs reacted (mean \pm 1 std. deviation) in UVPCO challenged with synthetic office VOC mixture and operated at approximately 595 m³/h (350 cfm) with two monolith configurations

Compound	<i>Exp 11</i> <i>Four 1-in Monoliths</i>		<i>Exp 8</i> <i>Eight 1-in Monoliths</i>	
	Mix Ratio (ppb)	<i>Reacted or Produced</i>	Mix Ratio (ppb)	<i>Reacted or Produced</i>
Ethanol	44 \pm 3	0.21 \pm 0.10	45 \pm 2	<i>Ns</i> *
MTBE	8.2 \pm 1.1	<i>Ns</i>	7.6 \pm 0.3	<i>Ns</i>
Isopropanol	29 \pm 2	0.33 \pm 0.11	30 \pm 2	0.29 \pm 0.11
1-Butanol	3.3 \pm 0.1	0.41 \pm 0.05	3.2 \pm 0.2	0.41 \pm 0.08
2-Butoxyethanol	7.0 \pm 0.1	0.59 \pm 0.02	6.9 \pm 0.2	0.80 \pm 0.03
2-Ethyl-1-hexanol	4.8 \pm 0.1	0.54 \pm 0.02	4.6 \pm 0.1	0.74 \pm 0.03
Phenol	1.88 \pm 0.17	0.62 \pm 0.12	2.0 \pm 0.1	0.83 \pm 0.08
Acetic acid	6.7	>0.55	12.6 \pm 4.6	>0.76
2-Butanone	3.1 \pm 0.1	0.07 \pm 0.04	3.0 \pm 0.1	<i>Ns</i>
MIBK	7.5 \pm 0.1	0.14 \pm 0.04	7.0 \pm 0.2	0.09 \pm 0.05
Hexanal	2.2 \pm 0.1	0.38 \pm 0.04	2.0 \pm 0.1	0.45 \pm 0.05
d-Limonene	3.9 \pm 0.1	0.39 \pm 0.05	3.7 \pm 0.2	0.57 \pm 0.08
Toluene	24 \pm 1	<i>Ns</i>	23 \pm 1	<i>Ns</i>
m-Xylene	7.3 \pm 0.1	0.09 \pm 0.02	7.4 \pm 0.2	0.13 \pm 0.04
1,2,4-TMB	2.2 \pm 0.1	0.27 \pm 0.01	2.2 \pm 0.1	0.41 \pm 0.04
n-Nonane	5.2 \pm 0.1	<i>Ns</i>	5.0 \pm 0.1	<i>Ns</i>
n-Decane	4.7 \pm 0.1	0.04 \pm 0.03	4.5 \pm 0.1	<i>Ns</i>
n-Undecane	4.1 \pm 0.1	0.06 \pm 0.03	4.0 \pm 0.1	<i>Ns</i>
n-Dodecane	11.3 \pm 0.1	0.11 \pm 0.02	10.8 \pm 0.2	0.08 \pm 0.03
R-11	5.9 \pm 0.8	<i>Ns</i>	5.6 \pm 0.2	<i>Ns</i>
Dichloromethane	27 \pm 1	<i>Ns</i>	25 \pm 1	<i>Ns</i>
1,1,1-TCA	15.9 \pm 3.2	<i>Ns</i>	13.9 \pm 1.8	<i>Ns</i>
Trichloroethene	2.0 \pm 0.1	<i>Ns</i>	1.87 \pm 0.05	<i>Ns</i>
PCE	4.8 \pm 0.1	<i>Ns</i>	4.6 \pm 0.1	<i>Ns</i>
1,2-DCB	1.47 \pm 0.01	<i>Ns</i>	1.42 \pm 0.04	<i>Ns</i>
Carbon disulfide	2.9 \pm 0.1	0.13 \pm 0.10	2.7 \pm 0.3	<i>Ns</i>
D5	1.74 \pm 0.02	0.34 \pm 0.02	1.65 \pm 0.04	0.36 \pm 0.05

**Ns* = Difference between upstream and downstream VOC concentration not significant at 95% confidence level by 1-tailed Student's t test

Table 6. VOC reaction rates in $\mu\text{mole VOC per hour}$ and $\mu\text{mole carbon per hour}$ (mean \pm 1 std. deviation) in UVPCO challenged with synthetic office VOC mixture and operated at approximately $170 \text{ m}^3/\text{h}$ (100 cfm) with three monolith configurations

Compound	<i>Exp 12 Four 0.5-in Monoliths</i>		<i>Exp 10 Four 1-in Monoliths</i>		<i>Exp 9 Eight 1-in Monoliths</i>	
	$\mu\text{mole/h}$	$\mu\text{moleC/h}$	$\mu\text{mole/h}$	$\mu\text{moleC/h}$	$\mu\text{mole/h}$	$\mu\text{moleC/h}$
Ethanol	260 \pm 20	520 \pm 40	190 \pm 35	380 \pm 70	280 \pm 10	550 \pm 20
MTBE	15.3 \pm 9.0	76 \pm 45	23 \pm 13	117 \pm 67	17.0 \pm 11.2	85 \pm 56
Isopropanol	195 \pm 26	590 \pm 80	166 \pm 29	500 \pm 90	220 \pm 10	670 \pm 40
1-Butanol	16.6 \pm 1.3	66 \pm 5	21 \pm 1	83 \pm 5	25 \pm 1	101 \pm 2
2-Butoxyethanol	36 \pm 1	220 \pm 10	45 \pm 1	270 \pm 10	54 \pm 1	320 \pm 10
2-Ethyl-1-hexanol	24 \pm 1	190 \pm 10	29 \pm 1	230 \pm 10	35 \pm 1	280 \pm 10
Phenol	11.5 \pm 1.8	69 \pm 11	11.6 \pm 0.8	69 \pm 4	14.0 \pm 0.3	84 \pm 2
Acetic acid	>35	>70	>35	>70	*	
2-Butanone	4.0 \pm 1.9	16.2 \pm 7.7			6.3 \pm 2.1	25 \pm 8
MIBK	22 \pm 3	134 \pm 20	26 \pm 3	159 \pm 17	35 \pm 2	210 \pm 10
Hexanal	8.4 \pm 1.0	51 \pm 6	10.9 \pm 0.6	65 \pm 4	13.3 \pm 0.7	80 \pm 4
d-Limonene	19.1 \pm 1.5	191 \pm 15	19.7 \pm 1.5	197 \pm 15	28 \pm 1	280 \pm 10
Toluene			8.4 \pm 6.4	59 \pm 45	14.3 \pm 5.9	100 \pm 41
m-Xylene	9.4 \pm 3.3	76 \pm 26	27 \pm 2	210 \pm 20	41 \pm 2	330 \pm 20
1,2,4-TMB	7.3 \pm 0.2	66 \pm 2	11.8 \pm 0.4	106 \pm 4	15.7 \pm 0.4	141 \pm 4
n-Nonane			2.7 \pm 1.0	24 \pm 9	4.7 \pm 1.9	43 \pm 17
n-Decane	4.0 \pm 0.6	40 \pm 6	5.1 \pm 1.1	51 \pm 11	8.2 \pm 1.9	82 \pm 19
n-Undecane	7.6 \pm 0.3	83 \pm 4	8.5 \pm 1.1	93 \pm 12	13.3 \pm 1.7	146 \pm 18
n-Dodecane	29 \pm 3	350 \pm 30	35 \pm 3	420 \pm 40	51 \pm 4	610 \pm 40

Table 6. Continued.

Compound	<i>Exp 12 Four 0.5-in Monoliths</i>		<i>Exp 10 Four 1-in Monoliths</i>		<i>Exp 9 Eight 1-in Monoliths</i>	
	$\mu\text{mole/h}$	$\mu\text{moleC/h}$	$\mu\text{mole/h}$	$\mu\text{moleC/h}$	$\mu\text{mole/h}$	$\mu\text{moleC/h}$
R-11					7.0±5.4	7.0±5.4
Dichloromethane						
1,1,1-TCA						
Trichloroethene						
PCE						
1,2-DCB			0.4±0.3	2.6±1.7		
Carbon disulfide	5.1±3.8	5.1±3.8				
D5	5.8±0.9	58±9	8.5±0.4	85±4	11.4±0.4	114±4

*Value not shown if difference between upstream and downstream VOC concentration was not significant at 95% confidence level by 1-tailed Student's t test

Table 7. VOC reaction rates in $\mu\text{mole VOC per hour}$ and $\mu\text{mole carbon per hour}$ (mean \pm 1 std. deviation) in UVPCO challenged with synthetic office VOC mixture and operated at approximately $170 \text{ m}^3/\text{h}$ (100 cfm) with two monolith configurations

Compound	<i>Exp 11</i> <i>Four 1-in Monoliths</i>		<i>Exp 8</i> <i>Eight 1-in Monoliths</i>	
	$\mu\text{mole/h}$	$\mu\text{moleC/h}$	$\mu\text{mole/h}$	$\mu\text{moleC/h}$
Ethanol	220 \pm 100	430 \pm 210	*	
MTBE				
Isopropanol	230 \pm 70	680 \pm 220	210 \pm 80	620 \pm 230
1-Butanol	33 \pm 4	131 \pm 15	32 \pm 6	129 \pm 25
2-Butoxyethanol	99 \pm 3	590 \pm 20	135 \pm 4	810 \pm 20
2-Ethyl-1-hexanol	62 \pm 2	490 \pm 20	83 \pm 3	660 \pm 20
Phenol	28 \pm 5	169 \pm 30	41 \pm 3	240 \pm 20
Acetic acid	>89	>178	>230	>470
2-Butanone	5.4 \pm 3.0	22 \pm 12		
MIBK	25 \pm 7	149 \pm 42	15.4 \pm 8.8	93 \pm 53
Hexanal	19.5 \pm 2.1	117 \pm 13	22 \pm 3	135 \pm 15
d-Limonene	36 \pm 5	360 \pm 50	51 \pm 6	510 \pm 60
Toluene				
m-Xylene	16.5 \pm 4.2	132 \pm 34	23 \pm 8	186 \pm 61
1,2,4-TMB	14.2 \pm 0.7	128 \pm 6	22 \pm 2	195 \pm 20
n-Nonane				
n-Decane	3.9 \pm 2.9	39 \pm 29		
n-Undecane	6.1 \pm 2.7	67 \pm 30		
n-Dodecane	30 \pm 7	360 \pm 80	20 \pm 7	240 \pm 80
R-11				
Dichloromethane				
1,1,1-TCA				
Trichloroethene				
PCE				
1,2-DCB				
Carbon disulfide	8.9 \pm 7.0	8.9 \pm 7.0		
D5	14.1 \pm 0.8	141 \pm 8	14.6 \pm 1.8	146 \pm 18

*Value not shown if difference between upstream and downstream VOC concentration was not significant at 95% confidence level by 1-tailed Student's t test

Table 8. Downstream mixing ratios and differences between downstream and upstream mixing ratios (ppb) of formaldehyde, acetaldehyde, and acetone (mean \pm 1 std. deviation) in UVPCO challenged with synthetic office VOC mixture and operated at approximately 170 m³/h (100 cfm) with three monolith configurations

Compound	<i>Exp 12 Four 0.5-in Monoliths</i>		<i>Exp 10 Four 1-in Monoliths</i>		<i>Exp 9 Eight 1-in Monoliths</i>	
	Downstr. Mix Ratio (ppb)	Increase in Mix Ratio (ppb)	Downstr. Mix Ratio (ppb)	Increase in Mix Ratio (ppb)	Downstr. Mix Ratio (ppb)	Increase in Mix Ratio (ppb)
Formaldehyde	4.0 \pm 0.1	1.19 \pm 0.15	4.3 \pm 0.3	2.1 \pm 0.3	2.6 \pm 0.2	Ns*
Acetaldehyde	24 \pm 1	21 \pm 1	25 \pm 1	24 \pm 1	27 \pm 1	25 \pm 1
Acetone	63 \pm 1	20 \pm 1	65 \pm 2	21 \pm 1	61 \pm 1	23 \pm 1

*Ns = Difference between upstream and downstream VOC concentration not significant at 95% confidence level by 1-tailed Student's t test

Table 9. Downstream mixing ratios and differences between downstream and upstream mixing ratios (ppb) of formaldehyde, acetaldehyde, and acetone (mean \pm 1 std. deviation) in UVPCO challenged with synthetic office VOC mixture and operated at approximately 595 m³/h (350 cfm) with two monolith configurations

Compound	<i>Exp 11 Four 1-in Monoliths</i>		<i>Exp 8 Eight 1-in Monoliths</i>	
	Downstr. Mix Ratio (ppb)	Increase in Mix Ratio (ppb)	Downstr. Mix Ratio (ppb)	Increase in Mix Ratio (ppb)
Formaldehyde	6.2 \pm 0.1	3.8 \pm 0.2	7.4 \pm 0.8	3.0 \pm 0.8
Acetaldehyde	9.7 \pm 0.9	7.9 \pm 0.9	8.9 \pm 1.6	7.0 \pm 1.7
Acetone	47 \pm 2	7.5 \pm 2.2	35 \pm 5	8.4 \pm 5.7

Table 10. Production rates of formaldehyde, acetaldehyde, and acetone in $\mu\text{mole VOC}$ per hour and $\mu\text{mole carbon}$ per hour (mean \pm 1 std. deviation) in UVPCO challenged with synthetic office VOC mixture and operated at approximately $170 \text{ m}^3/\text{h}$ (100 cfm) with three monolith configurations

Compound	<i>Exp 12</i> <i>Four 0.5-in Monoliths</i>		<i>Exp 10</i> <i>Four 1-in Monoliths</i>		<i>Exp 9</i> <i>Eight 1-in Monoliths</i>	
	$\mu\text{mole/h}$	$\mu\text{moleC/h}$	$\mu\text{mole/h}$	$\mu\text{moleC/h}$	$\mu\text{mole/h}$	$\mu\text{moleC/h}$
Formaldehyde	8.2 \pm 1.0	8.2 \pm 1.0	15.2 \pm 2.2	15.2 \pm 2.2	*	
Acetaldehyde	147 \pm 3	290 \pm 10	169 \pm 9	340 \pm 20	177 \pm 10	350 \pm 20
Acetone	140 \pm 7	420 \pm 20	151 \pm 16	450 \pm 50	166 \pm 6	500 \pm 20

*Value not shown if difference between upstream and downstream VOC concentration was not significant at 95% confidence level by 1-tailed Student's t test

Table 11. Production rates of formaldehyde, acetaldehyde, and acetone in $\mu\text{mole VOC}$ per hour and $\mu\text{mole carbon}$ per hour (mean \pm 1 std. deviation) in UVPCO challenged with synthetic office VOC mixture and operated at approximately $170 \text{ m}^3/\text{h}$ (100 cfm) with two monolith configurations

Compound	<i>Exp 11</i> <i>Four 1-in Monoliths</i>		<i>Exp 8</i> <i>Eight 1-in Monoliths</i>	
	$\mu\text{mole/h}$	$\mu\text{moleC/h}$	$\mu\text{mole/h}$	$\mu\text{moleC/h}$
Formaldehyde	92 \pm 4	92 \pm 4	73 \pm 20	73 \pm 20
Acetaldehyde	191 \pm 21	380 \pm 40	172 \pm 41	340 \pm 80
Acetone	181 \pm 52	540 \pm 160	210 \pm 140	620 \pm 420

Table 12. Downstream VOC mixing ratios (ppb) and fractions of VOCs reacted (mean \pm 1 std. deviation) in UVPCO challenged with VOC mixture generated in 20-m³ chamber with combination of building products. UVPCO was operated at 168 – 173 m³/h (99 – 104 cfm) with three lamp configurations and at 303 m³/h (178 cfm) with all nine lamps

Compound	<i>Exp 18, 3 Lamps 168 m³/h</i>		<i>Exp 17, 6 Lamps 168 m³/h</i>		<i>Exp 15, 9 Lamps 176 m³/h</i>		<i>Exp 16, 9 Lamps 303 m³/h</i>	
	Mix Ratio (ppb)	<i>Fraction Reacted*</i>	Mix Ratio (ppb)	<i>Fraction Reacted</i>	Mix Ratio (ppb)	<i>Fraction Reacted</i>	Mix Ratio (ppb)	<i>Fraction Reacted</i>
Phenol	12.1 \pm 0.1	0.83 \pm 0.01	12.5 \pm 0.5	0.88 \pm 0.05	11.2 \pm 0.4	0.87 \pm 0.05	8.3 \pm 0.2	0.76 \pm 0.03
BHT	0.4 \pm 0.1	0.75 \pm 0.32	0.7 \pm 0.1	0.67 \pm 0.25	0.7 \pm 0.1	0.66 \pm 0.21	0.7 \pm 0.1	0.55 \pm 0.21
Ethylene glycol	80 \pm 17	0.86 \pm 0.28	104 \pm 4	0.89 \pm 0.05	108 \pm 7	0.89 \pm 0.09	92 \pm 13	0.91 \pm 0.19
DEGBE	12.8 \pm 0.5	0.76 \pm 0.06	16.1 \pm 0.7	0.82 \pm 0.05	19.5 \pm 0.3	0.82 \pm 0.02	14.4 \pm 0.5	0.68 \pm 0.04
Acetic acid	25 \pm 2	-0.70 \pm 0.10	32 \pm 1	<i>Ns**</i>	28 \pm 3	0.47 \pm 0.12	25 \pm 2	0.34 \pm 0.09
Hexanal	1.5 \pm 0.3	-0.38 \pm 0.29	1.6 \pm 0.1	<i>Ns</i>	1.3 \pm 0.2	<i>Ns</i>	1.0 \pm 0.1	0.11 \pm 0.07
TMPD-MIB	11.7 \pm 0.3	0.70 \pm 0.03	13.8 \pm 0.3	0.77 \pm 0.03	16.0 \pm 0.3	0.76 \pm 0.03	11.3 \pm 0.3	0.63 \pm 0.04
TMPD-DIB	27 \pm 1	0.54 \pm 0.01	28 \pm 1	0.65 \pm 0.04	26 \pm 1	0.65 \pm 0.05	18.3 \pm 0.5	0.49 \pm 0.04
Toluene	1.8 \pm 0.2	<i>Ns</i>	0.7 \pm 0.2	<i>Ns</i>	1.0 \pm 0.1	<i>Ns</i>	1.4 \pm 0.8	<i>Ns</i>
1,2,4-TMB	1.2 \pm 0.1	0.06 \pm 0.02	1.2 \pm 0.1	0.14 \pm 0.05	1.1 \pm 0.1	0.14 \pm 0.04	0.8 \pm 0.1	0.12 \pm 0.06
C ₄ Alkylbenzenes	4.8 \pm 0.1	0.08 \pm 0.03	5.0 \pm 0.1	0.23 \pm 0.05	4.3 \pm 0.1	0.31 \pm 0.04	3.1 \pm 0.1	0.22 \pm 0.06
Naphthalene	0.05 \pm 0.0	0.17 \pm 0.01	0.5 \pm 0.1	0.34 \pm 0.06	0.5 \pm 0.0	0.38 \pm 0.03	0.3 \pm 0.0	0.26 \pm 0.06
C ₁₀ Alkylbenzenes	7.4 \pm 0.1	0.30 \pm 0.01	8.0 \pm 0.1	0.49 \pm 0.04	7.5 \pm 0.3	0.56 \pm 0.04	5.5 \pm 0.2	0.41 \pm 0.05
C ₁₁ Alkylbenzenes	14.3 \pm 0.1	0.42 \pm 0.01	14.8 \pm 0.4	0.59 \pm 0.04	12.8 \pm 0.5	0.63 \pm 0.05	9.9 \pm 0.2	0.48 \pm 0.04
C ₁₂ Alkylbenzenes	5.2 \pm 0.1	0.50 \pm 0.01	5.3 \pm 0.1	0.63 \pm 0.03	4.3 \pm 0.2	0.66 \pm 0.06	3.5 \pm 0.1	0.52 \pm 0.04
C ₁₁ Alkane HCs	32 \pm 1	0.04 \pm 0.02	33 \pm 1	0.08 \pm 0.4	30 \pm 1	<i>Ns</i>	21 \pm 1	<i>Ns</i>
n-Undecane	1.1 \pm 0.1	<i>Ns</i>	1.2 \pm 0.1	<i>Ns</i>	0.8 \pm 0.1	<i>Ns</i>	0.5 \pm 0.1	<i>Ns</i>
n-Dodecane	4.5 \pm 0.1	0.06 \pm 0.02	4.9 \pm 0.1	0.13 \pm 0.04	4.4 \pm 0.1	0.11 \pm 0.03	3.2 \pm 0.1	0.08 \pm 0.05
n-Tridecane	14.5 \pm 0.3	0.11 \pm 0.02	15.8 \pm 0.4	0.20 \pm 0.05	14.5 \pm 0.5	0.22 \pm 0.04	10.4 \pm 0.3	0.15 \pm 0.05
n-Tetradecane	8.7 \pm 0.2	0.13 \pm 0.02	9.5 \pm 0.3	0.27 \pm 0.06	8.8 \pm 0.3	0.32 \pm 0.04	6.4 \pm 0.2	0.22 \pm 0.05

*Negative values for acetic acid and hexanal indicate net production

**Ns = Difference between upstream and downstream VOC concentration not significant at 95% confidence level by 1-tailed Student's t test

Table 13. VOC reaction rates in $\mu\text{mole VOC per hour}$ and $\mu\text{mole carbon per hour}$ (mean \pm 1 std. deviation) in UVPCO challenged with VOC mixture generated in 20- m^3 chamber with combination of building products. UVPCO was operated at 168 – 173 m^3/h (99 – 104 cfm) with three lamp configurations and at 303 m^3/h (178 cfm) with all nine lamps

Compound	<i>Exp 18, 3 Lamps*</i> <i>168 m³/h</i>		<i>Exp 17, 6 Lamps</i> <i>168 m³/h</i>		<i>Exp 15, 9 Lamps</i> <i>176 m³/h</i>		<i>Exp 16, 9 Lamps</i> <i>303 m³/h</i>	
	$\mu\text{mole/h}$	$\mu\text{moleC/h}$	$\mu\text{mole/h}$	$\mu\text{moleC/h}$	$\mu\text{mole/h}$	$\mu\text{moleC/h}$	$\mu\text{mole/h}$	$\mu\text{moleC/h}$
Phenol	69 \pm 1	420 \pm 10	75 \pm 4	450 \pm 20	70 \pm 3	420 \pm 20	79 \pm 3	470 \pm 20
BHT	2.0 \pm 0.7	30 \pm 10	3.0 \pm 0.9	46 \pm 14	3.2 \pm 0.9	48 \pm 13	4.9 \pm 1.8	74 \pm 26
Ethylene glycol	470 \pm 120	940 \pm 240	640 \pm 30	1280 \pm 60	690 \pm 50	1390 \pm 110	1040 \pm 160	2100 \pm 300
DEGBE	67 \pm 4	540 \pm 30	91 \pm 5	720 \pm 40	114 \pm 3	910 \pm 20	122 \pm 7	970 \pm 50
Acetic acid	-124 \pm 15	-248 \pm 30	**		93 \pm 21	187 \pm 42	105 \pm 29	210 \pm 60
Hexanal	-3.8 \pm 2.8	-23 \pm 17					1.3 \pm 0.9	7.7 \pm 5.4
TMPD-MIB	56 \pm 2	670 \pm 20	74 \pm 2	880 \pm 30	87 \pm 2	1050 \pm 30	88 \pm 5	1060 \pm 60
TMPD-DIB	99 \pm 2	1590 \pm 30	125 \pm 6	2000 \pm 100	119 \pm 8	1900 \pm 120	112 \pm 9	1790 \pm 140
Toluene								
1,2,4-TMB	0.5 \pm 0.1	4.9 \pm 1.2	1.2 \pm 0.5	10.6 \pm 4.1	1.1 \pm 0.3	10.1 \pm 2.6	1.2 \pm 0.5	10.6 \pm 4.9
C ₄ Alkylbenzenes	2.8 \pm 1.1	28 \pm 11	7.8 \pm 1.7	78 \pm 17	9.7 \pm 1.2	97 \pm 12	8.4 \pm 2.2	84 \pm 22
Naphthalene	0.6 \pm 0.1	6.0 \pm 0.5	1.2 \pm 0.2	12.2 \pm 2.2	1.3 \pm 0.1	12.5 \pm 1.1	1.1 \pm 0.3	11.0 \pm 2.5
C ₁₀ Alkylbenzenes	15.4 \pm 0.7	250 \pm 10	27 \pm 2	430 \pm 30	30 \pm 2	480 \pm 30	28 \pm 3	450 \pm 50
C ₁₁ Alkylbenzenes	41 \pm 1	700 \pm 10	60 \pm 4	1020 \pm 70	68 \pm 4	980 \pm 70	60 \pm 5	1010 \pm 80
C ₁₂ Alkylbenzenes	17.9 \pm 0.5	320 \pm 10	23 \pm 1	420 \pm 20	20 \pm 2	370 \pm 30	23 \pm 2	410 \pm 30
C ₁₁ Alkane HCs	9.2 \pm 4.8	101 \pm 53	17.6 \pm 9.7	194 \pm 107				
n-Undecane								
n-Dodecane	1.8 \pm 0.8	21 \pm 9	4.4 \pm 1.3	53 \pm 16	3.4 \pm 1.0	40 \pm 12	3.2 \pm 1.9	39 \pm 23
n-Tridecane	10.5 \pm 2.2	136 \pm 29	22 \pm 6	290 \pm 70	23 \pm 4	300 \pm 60	19.8 \pm 6.6	260 \pm 90
n-Tetradecane	7.8 \pm 1.2	109 \pm 16	17.4 \pm 3.6	240 \pm 50	21 \pm 2	290 \pm 30	17.3 \pm 4.1	240 \pm 60

*Negative values for acetic acid and hexanal indicate production rates

**Value not shown if difference between upstream and downstream VOC concentration was not significant at 95% confidence level by 1-tailed Student's t test

Table 14. Downstream mixing ratios and differences between downstream and upstream mixing ratios (ppb) of formaldehyde, acetaldehyde, and acetone (mean \pm 1 std. deviation) in UVPCO challenged with VOC mixture generated in 20-m³ chamber with combination of building products. UVPCO was operated at 168 – 173 m³/h (99 – 104 cfm) with three lamp configurations and at 303 m³/h (178 cfm) with all nine lamps

Compound	<i>Exp 18, 3 Lamps 168 m³/h</i>		<i>Exp 17, 6 Lamps 168 m³/h</i>		<i>Exp 15, 9 Lamps 176 m³/h</i>		<i>Exp 16, 9 Lamps 303 m³/h</i>	
	Downstr. Mix Ratio (ppb)	Increase in Mix Ratio (ppb)	Downstr. Mix Ratio (ppb)	Increase in Mix Ratio (ppb)	Downstr. Mix Ratio (ppb)	Increase in Mix Ratio (ppb)	Downstr. Mix Ratio (ppb)	Increase in Mix Ratio (ppb)
Formaldehyde	91 \pm 10	54 \pm 10	89 \pm 5	53 \pm 5	70 \pm 4	36 \pm 5	52 \pm 3	24 \pm 4
Acetaldehyde	13.2 \pm 1.8	8.8 \pm 1.8	18.6 \pm 1.3	13.4 \pm 1.3	20 \pm 1	14.6 \pm 1.4	12.6 \pm 1.0	7.5 \pm 1.3
Acetone	57 \pm 6	44 \pm 6	70 \pm 4	55 \pm 4	65 \pm 3	47 \pm 4	34 \pm 1	22 \pm 2

Table 15. Production rates of formaldehyde, acetaldehyde, and acetone in μ mole VOC per hour and μ mole carbon per hour (mean \pm 1 std. deviation) in UVPCO challenged with VOC mixture generated in 20-m³ chamber with combination of building products. UVPCO was operated at 168 – 173 m³/h (99 – 104 cfm) with three lamp configurations and at 303 m³/h (178 cfm) with all nine lamps

Compound	<i>Exp 18, 3 Lamps 168 m³/h</i>		<i>Exp 17, 6 Lamps 168 m³/h</i>		<i>Exp 15, 9 Lamps 176 m³/h</i>		<i>Exp 16, 9 Lamps 303 m³/h</i>	
	μ mole/h	μ moleC/h	μ mole/h	μ moleC/h	μ mole/h	μ moleC/h	μ mole/h	μ moleC/h
Formaldehyde	370 \pm 70	370 \pm 70	370 \pm 40	370 \pm 40	250 \pm 40	250 \pm 40	290 \pm 50	290 \pm 50
Acetaldehyde	60 \pm 13	121 \pm 25	92 \pm 9	184 \pm 19	104 \pm 10	210 \pm 20	93 \pm 16	185 \pm 32
Acetone	300 \pm 40	900 \pm 130	380 \pm 30	1130 \pm 80	340 \pm 30	1010 \pm 80	270 \pm 30	810 \pm 80

Table 16. Upstream and downstream formaldehyde, acetaldehyde, and acetone mixing ratios (ppb) (mean \pm 1 std. deviation) in UVPCO challenged with mixture of formaldehyde and acetaldehyde generated in 20-m³ chamber ventilated with room air. UVPCO was operated at 169 m³/h (99 cfm) with one inlet concentration and at approximately 290 m³/h (~171 cfm) with three inlet concentrations

Compound	<i>Exp 19, Low Conc 169 m³/h</i>		<i>Exp 20, Low Conc 294 m³/h</i>		<i>Exp 21, Mid Conc 299 m³/h</i>		<i>Exp 22, High Conc 280 m³/h</i>	
	Upstream Mix Ratio (ppb)	<i>Downstr. Mix Ratio (ppb)</i>	Upstream Mix Ratio (ppb)	<i>Downstr. Mix Ratio (ppb)</i>	Upstream Mix Ratio (ppb)	<i>Downstr. Mix Ratio (ppb)</i>	Upstream Mix Ratio (ppb)	<i>Downstr. Mix Ratio (ppb)</i>
	<i>VOCs Reacted</i>							
Formaldehyde	30 \pm 3	2.4 \pm 0.1	24 \pm 3	7.9 \pm 0.4	56 \pm 5	36 \pm 3	88 \pm 8	38 \pm 2
Acetaldehyde	8.9 \pm 0.9	6.0 \pm 0.2	9.1 \pm 0.9	<i>Ns*</i>	17.7 \pm 1.4	<i>Ns</i>	23 \pm 2	<i>Ns</i>
	<i>VOC Produced</i>							
Acetone	2.1 \pm 0.2	3.5 \pm 0.1	3.0 \pm 0.2	4.5 \pm 0.1	4.7 \pm 0.3	8.4 \pm 0.6	2.8 \pm 0.1	4.6 \pm 0.1

*Ns = Difference between upstream and downstream VOC concentration not significant at 95% confidence level by 1-tailed Student's t test

Table 17. Formaldehyde, acetaldehyde, and acetone reaction rates in $\mu\text{mole VOC per hour}$ and $\mu\text{mole carbon per hour}$ (mean \pm 1 std. deviation) in UVPCO challenged with mixture of formaldehyde and acetaldehyde generated in 20-m³ chamber ventilated with room air. UVPCO was operated at 169 m³/h (99 cfm) with one inlet concentration and at approximately 290 m³/h (~171 cfm) with three inlet concentrations

Compound	<i>Exp 19, Low Conc 169 m³/h</i>		<i>Exp 20, Low Conc 294 m³/h</i>		<i>Exp 21, Mid Conc 299 m³/h</i>		<i>Exp 22, High Conc 280 m³/h</i>	
	$\mu\text{mole/h}$	$\mu\text{moleC/h}$	$\mu\text{mole/h}$	$\mu\text{moleC/h}$	$\mu\text{mole/h}$	$\mu\text{moleC/h}$	$\mu\text{mole/h}$	$\mu\text{moleC/h}$
	<i>VOCs Reacted</i>							
Formaldehyde	189 \pm 18	189 \pm 18	196 \pm 38	196 \pm 38	250 \pm 70	250 \pm 70	570 \pm 100	570 \pm 100
Acetaldehyde	19.9 \pm 6.1	40 \pm 12	*					
	<i>VOC Produced</i>							
Acetone	10.0 \pm 1.6	30 \pm 5	17.8 \pm 3.1	54 \pm 9	45 \pm 8	136 \pm 24	20 \pm 2	60 \pm 6

*Value not shown if difference between upstream and downstream VOC concentration was not significant at 95% confidence level by 1-tailed Student's t test or was $\leq 5\%$

Table 18. Target VOCs ordered by decreasing percent conversion efficiency (% Eff) in low flow rate (~175 m³/h) Exps 10, 15, and 19 with synthetic office VOC, building product, and aldehyde mixtures, respectively. Six VOCs occurred in both mixtures

Compound	Chem Class	% Eff	Compound	Chem Class	% Eff
Formaldehyde	Aldehyde	92	Naphthalene	Aromatic HC	38
Ethylene glycol	Glycol ether	89	MTBE	Ether	37
Phenol ^b	Alcohol	87	Acetaldehyde	Aldehyde	32
Phenol ^a	Alcohol	85	n-Tetradecane	Alkane HC	32
2-BE	Glycol ether	85	C ₄ Alkylbenzenes	Aromatic HC	31
DEGBE	Glycol ether	82	n-Undecane ^a	Alkane HC	27
Ethylhexanol	Alcohol	81	1,1,1-TCA	Halo HC	24
1-Butanol	Alcohol	79	n-Tridecane	Alkane HC	22
TMPD-MIB	Ester	76	R-11	Halo HC	20
Limonene	Terpene HC	75	n-Decane	Alkane HC	14
1,2,4-TMB ^a	Aromatic HC	70	1,2,4-TMB ^b	Aromatic HC	14
Hexanal ^a	Aldehyde	70	n-Dodecane ^b	Alkane HC	11
Isopropanol	Alcohol	67	DCM	Halo HC	<10
BHT	Alcohol	66	n-Nonane	Alkane HC	<10
C ₁₂ Alkylbenzenes	Aromatic HC	66	2-Butanone	Ketone	<10
TMPD-DIB	Ester	65	Toluene ^a	Aromatic HC	<10
D5	Siloxane	64	1,2-DCB	Halo HC	<10
C ₁₁ Alkylbenzenes	Aromatic HC	63	C ₁₁ Alkane HCs	Alkane HC	<10
C ₁₀ Alkylbenzenes	Aromatic HC	56	PCE	Halo HC	<10
Ethanol	Alcohol	53	Trichloroethene	Halo HC	<10
Acetic acid	Acid	47	u-Undecane ^b	Alkane HC	<10
MIBK	Ketone	46	CS ₂	Sulfide	<10
m-Xylene	Aromatic HC	46	Hexanal ^b	Aldehyde	<10
n-Dodecane ^a	Alkane HC	41	Toluene ^b	Aromatic HC	<10

a. Synthetic office VOC mixture

b. Building product mixture

Table 19. Measured and predicted effect of monolith thickness on reaction efficiency of phenol and limonene in experiments conducted at 168 – 175 m³/h with synthetic office VOC mixture

Exp No	Monolith Configuration	<i>Reaction Efficiency, %</i>			
		Phenol		Limonene	
		Measured	Predicted	Measured	Predicted
12	4 x 0.5-in	77±15	70	59±5	59
10	4 x 1-in	85±7	85	75±6	75
9	8 x 1-in	95±2	92	94±6	84

Table 20. Measured and predicted effect of UV power on reaction efficiency of C₁₀ alkylbenzenes in experiments conducted at 168 – 175 m³/h with building products mixture of VOCs

Exp No	No. Lamps	<i>Reaction Efficiency, %</i>	
		Measured	Predicted
18	3	30±1	33
17	6	49±4	48
15	9	56±4	55

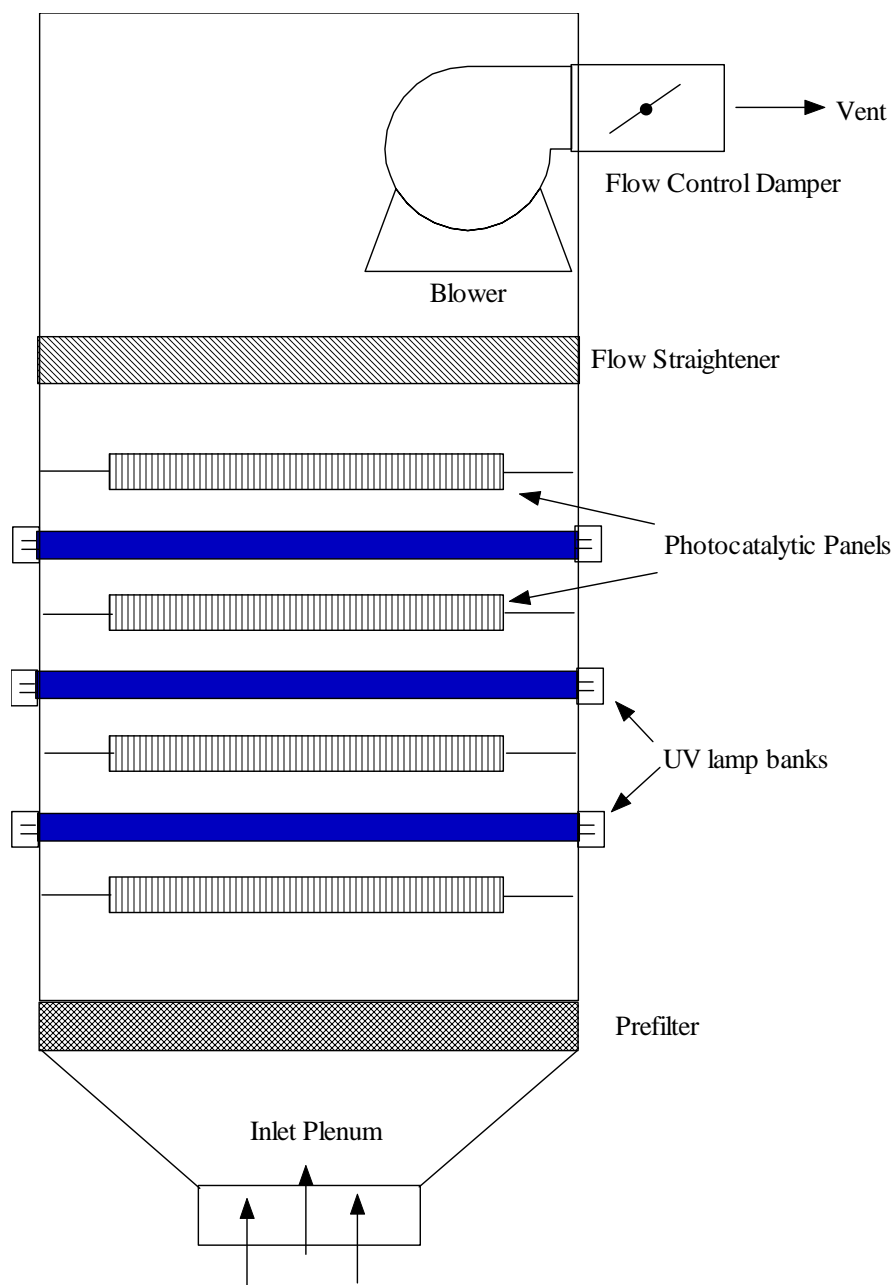


Figure 1. Schematic diagram of UVPCO reactor showing arrangement of four photocatalytic monoliths and three banks of three UVA lamps.

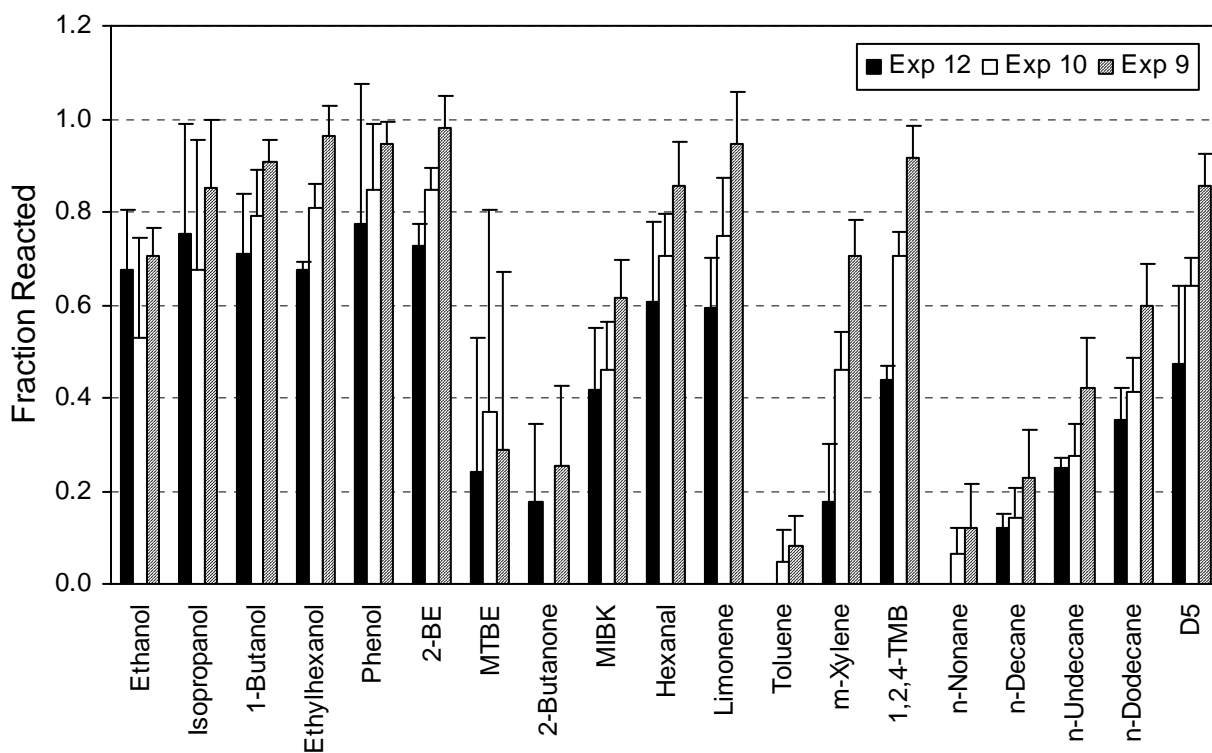


Figure 2. Mean fractions of VOCs reacted in three low flow rate ($\sim 170 \text{ m}^3/\text{h}$) experiments with synthetic office VOC mixture in which monolith thickness was varied. Experiment 12 had four 0.5-in monoliths; Experiment 10 had four 1-in monoliths; and Experiment 9 had eight 1-in monoliths. Error bars indicate two standard deviations of the means.

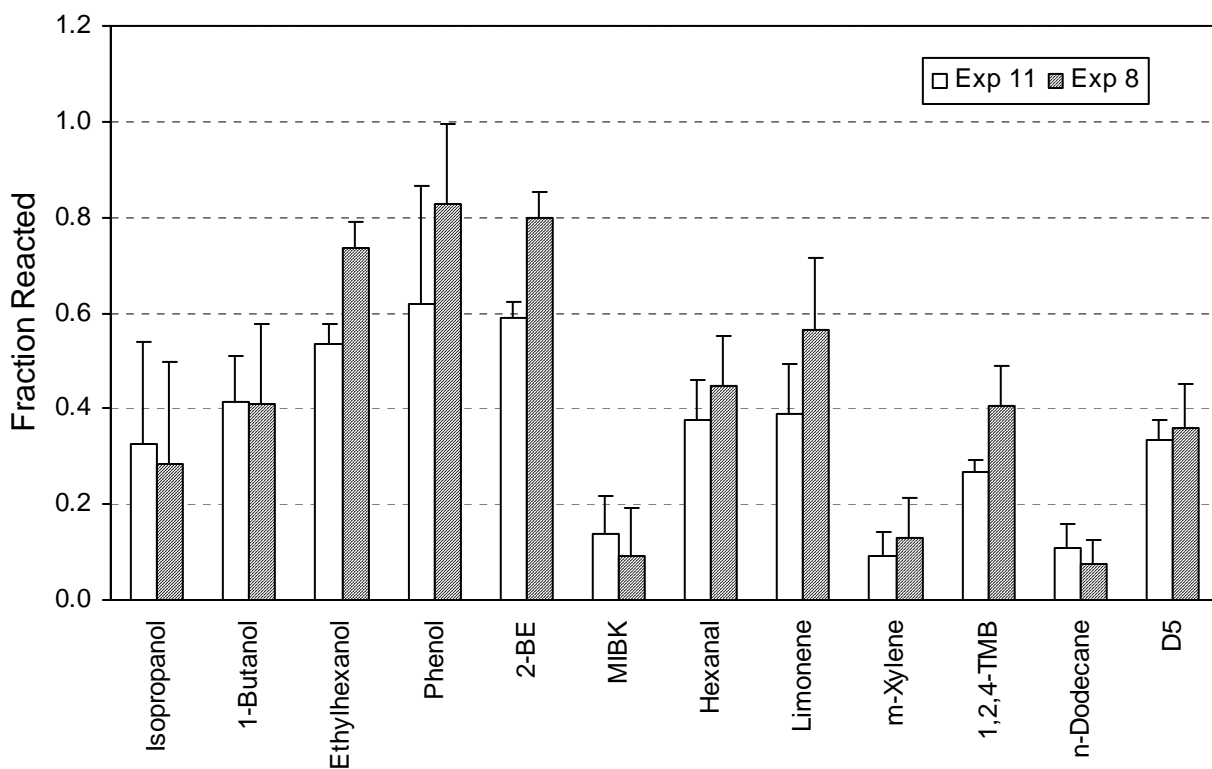


Figure 3. Mean fractions of VOCs reacted in two high flow rate ($\sim 595 \text{ m}^3/\text{h}$) experiments with synthetic office VOC mixture in which monolith thickness was varied. Experiment 11 had four 1-in monoliths; and Experiment 8 had eight 1-in monoliths. Error bars indicate two standard deviations of the means.

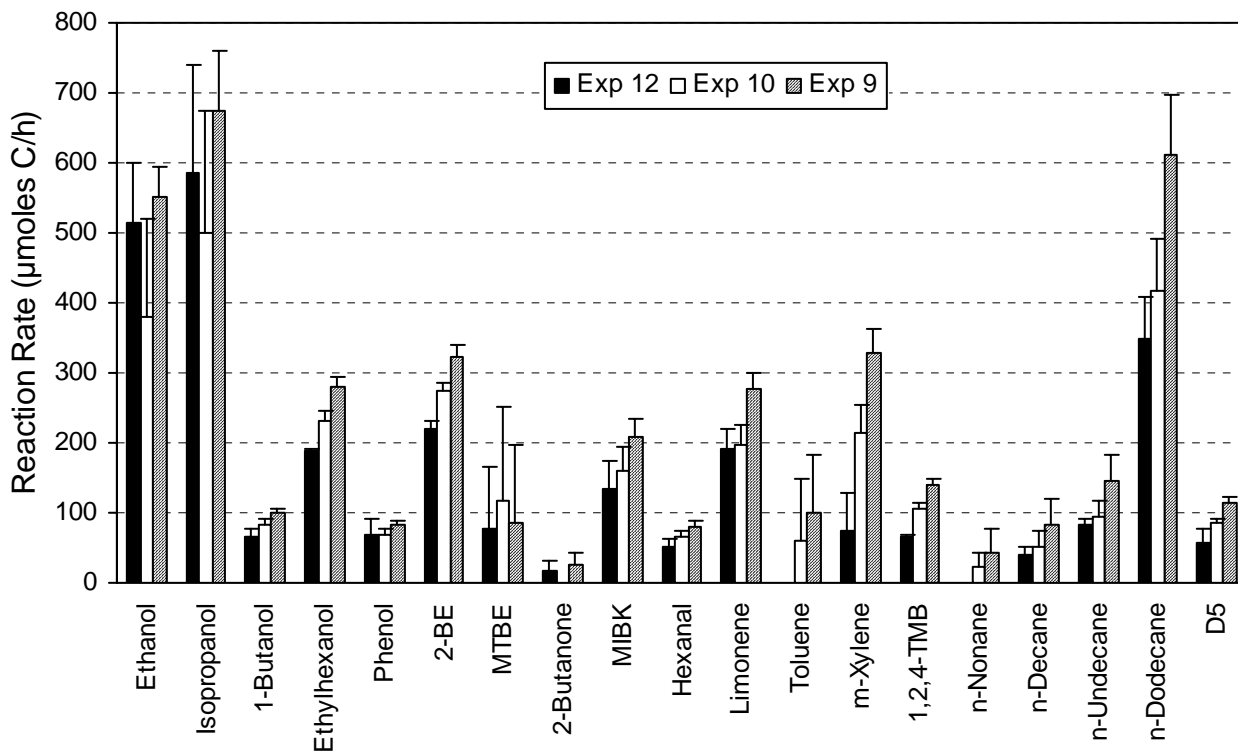


Figure 4. Mean VOC reaction rates ($\mu\text{mole carbon per hour}$) in three low flow rate ($\sim 170 \text{ m}^3/\text{h}$) experiments with synthetic office VOC mixture in which monolith thickness was varied. Experiment 12 had four 0.5-in monoliths; Experiment 10 had four 1-in monoliths; and Experiment 9 had eight 1-in monoliths. Error bars indicate two standard deviations of the means.

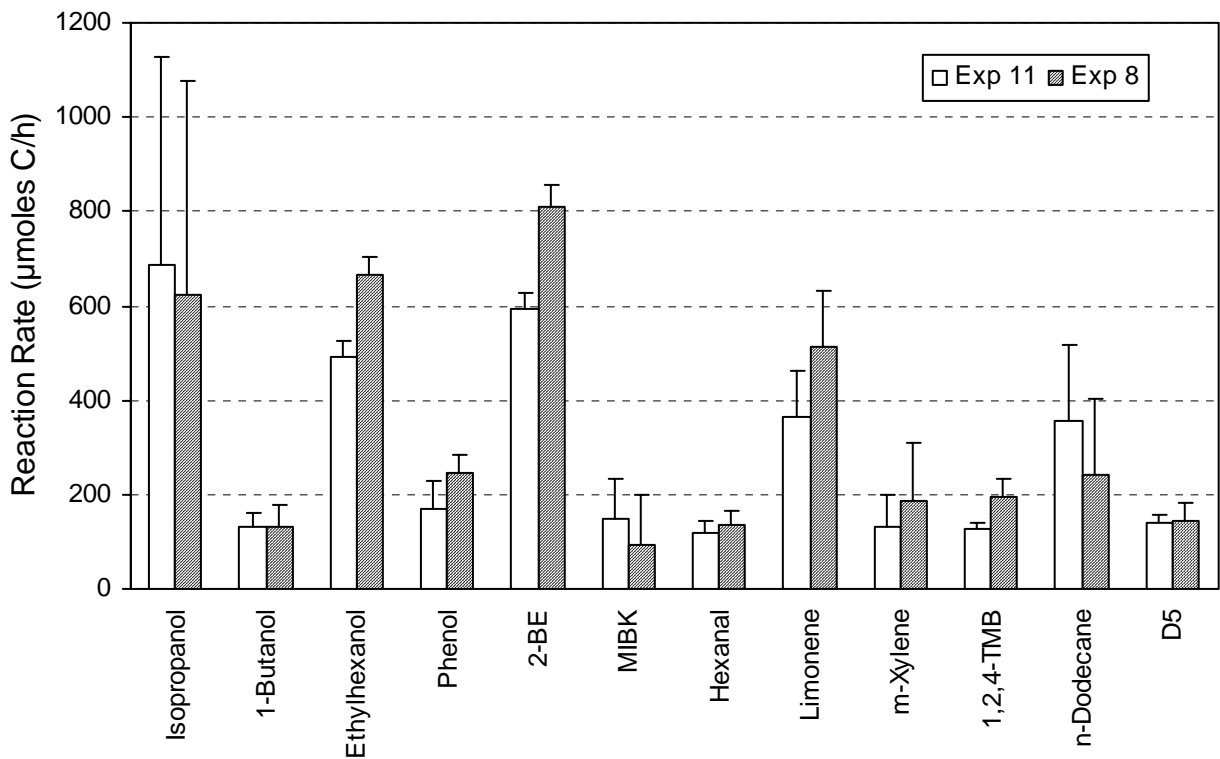


Figure 5. Mean VOC reaction rates ($\mu\text{mole carbon per hour}$) in two high flow rate ($\sim 595 \text{ m}^3/\text{h}$) experiments with synthetic office VOC mixture in which monolith thickness was varied. Experiment 11 had four 1-in monoliths; and Experiment 8 had eight 1-in monoliths. Error bars indicate two standard deviations of the means.

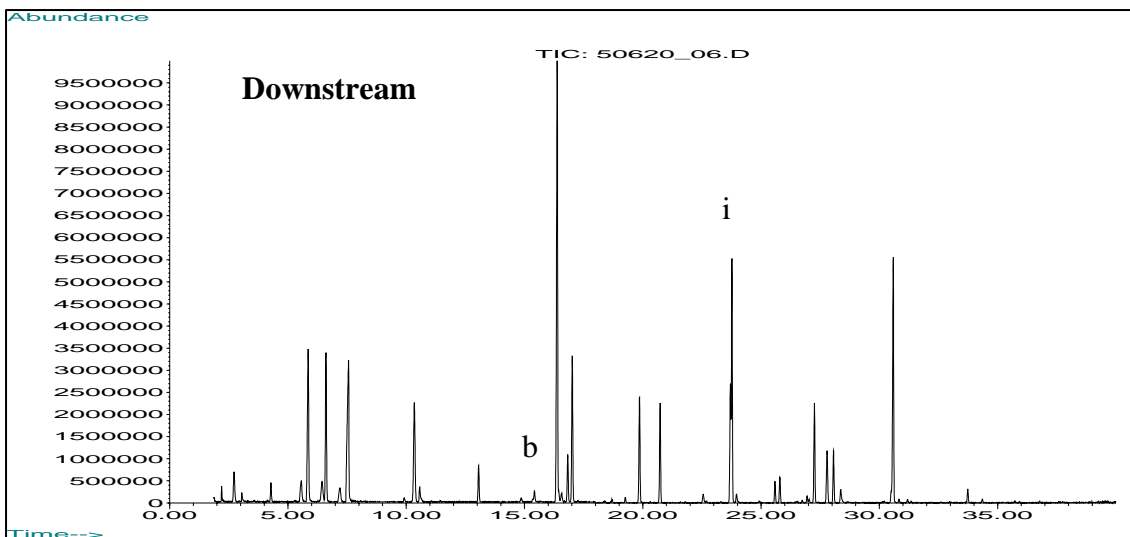
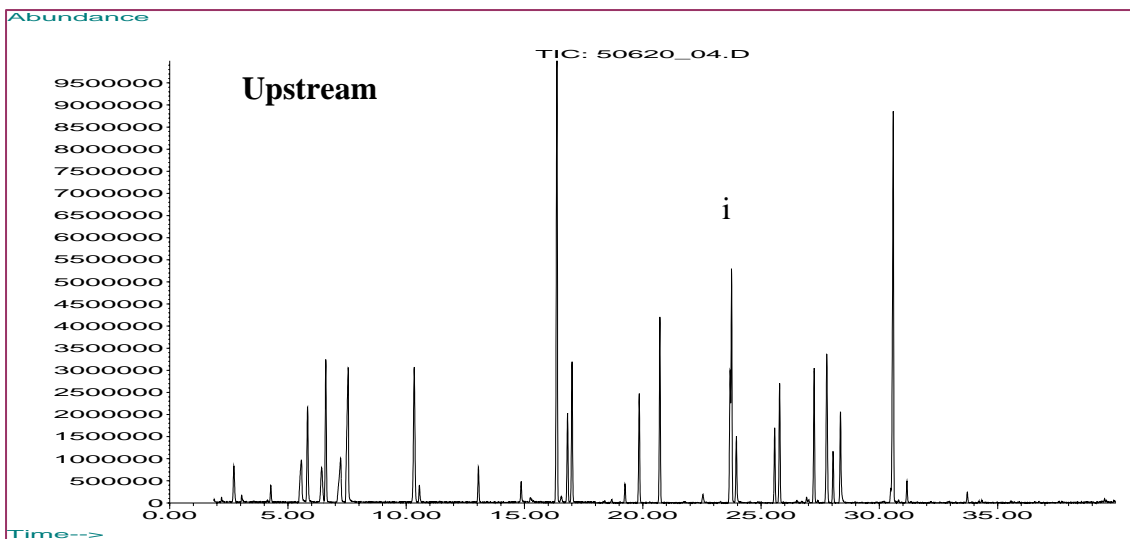


Figure 6. Comparison of total-ion-current chromatograms obtained by TD-GC/MS analysis of air samples collected upstream and downstream of UVPCO reactor in Experiment 10 with synthetic office VOC mixture. Production of butyl formate is indicated in downstream sample. b = Butyl formate; i = Internal standard.

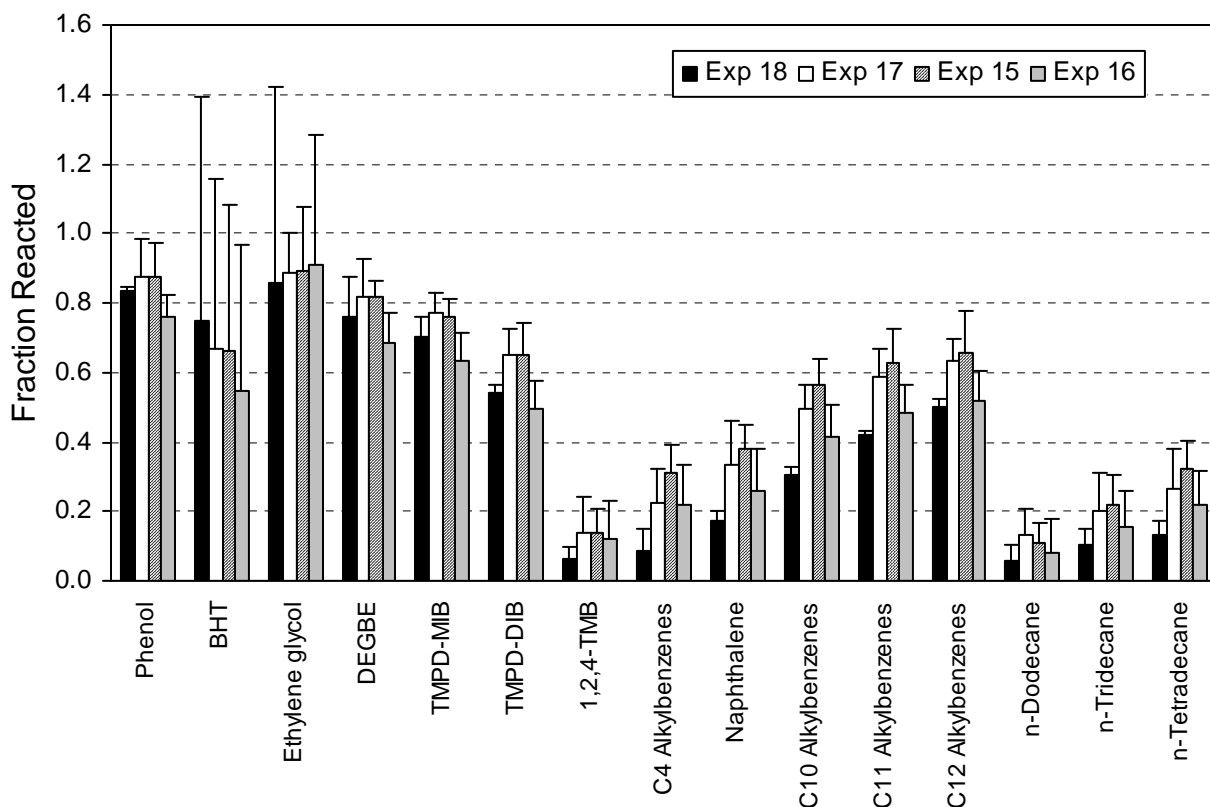


Figure 7. Mean fractions of VOCs reacted in four experiments with building product mixture in which device flow rate and the number of lamps were varied. Experiments 15, 17, and 18 were conducted at $\sim 168 \text{ m}^3/\text{h}$; Experiment 16 was conducted at $303 \text{ m}^3/\text{h}$. Experiment 18 had 3 lamps; Experiment 17 had six lamps; Experiments 15 and 16 had nine lamps. Error bars indicate two standard deviations of the means.

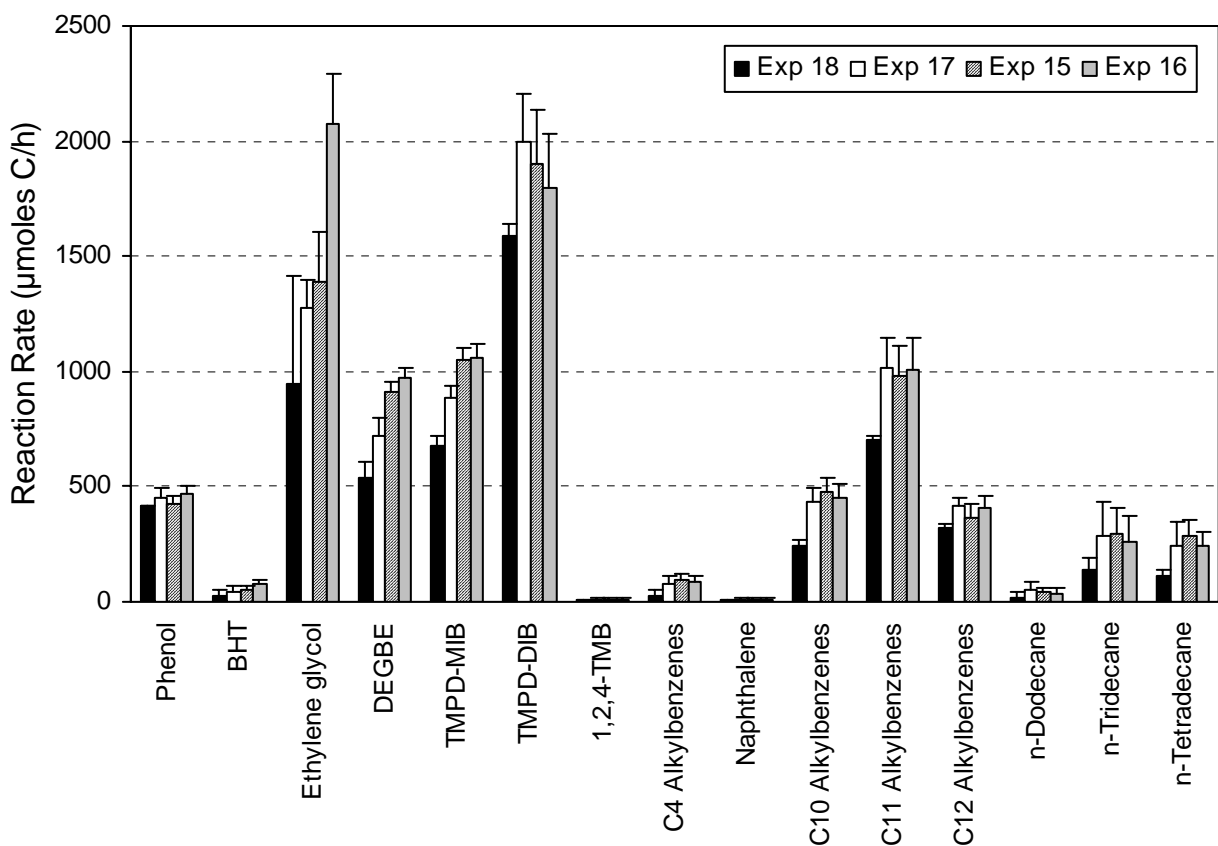


Figure 8. Mean VOC reaction rates in four experiments with building product mixture in which device flow rate and the number of lamps were varied. Experiments 15, 17, and 18 were conducted at $\sim 168 \text{ m}^3/\text{h}$; Experiment 16 was conducted at $303 \text{ m}^3/\text{h}$. Experiment 18 had 3 lamps; Experiment 17 had six lamps; Experiments 15 and 16 had nine lamps. Error bars indicate two standard deviations of the means.

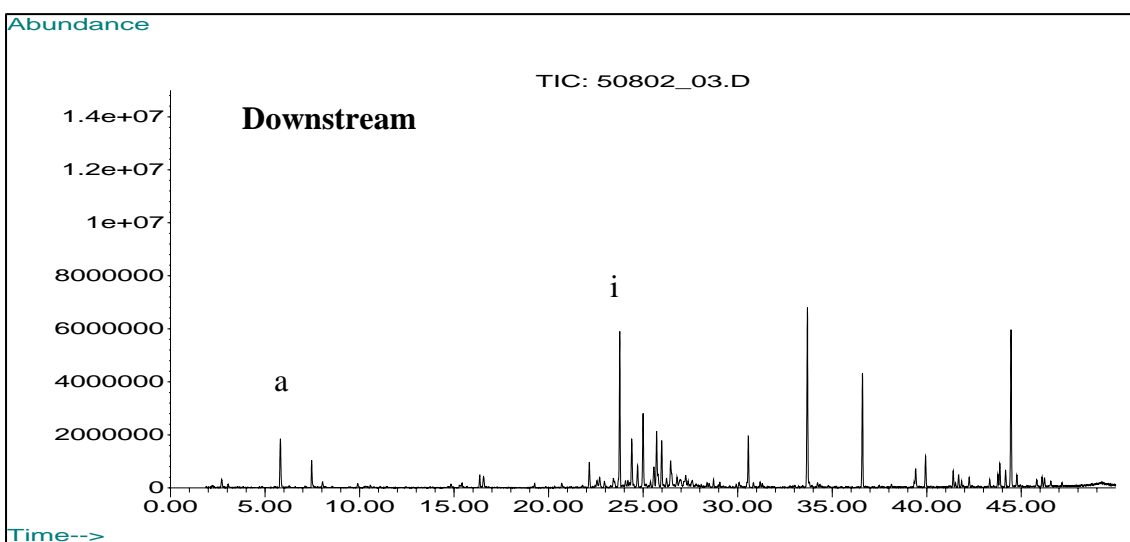
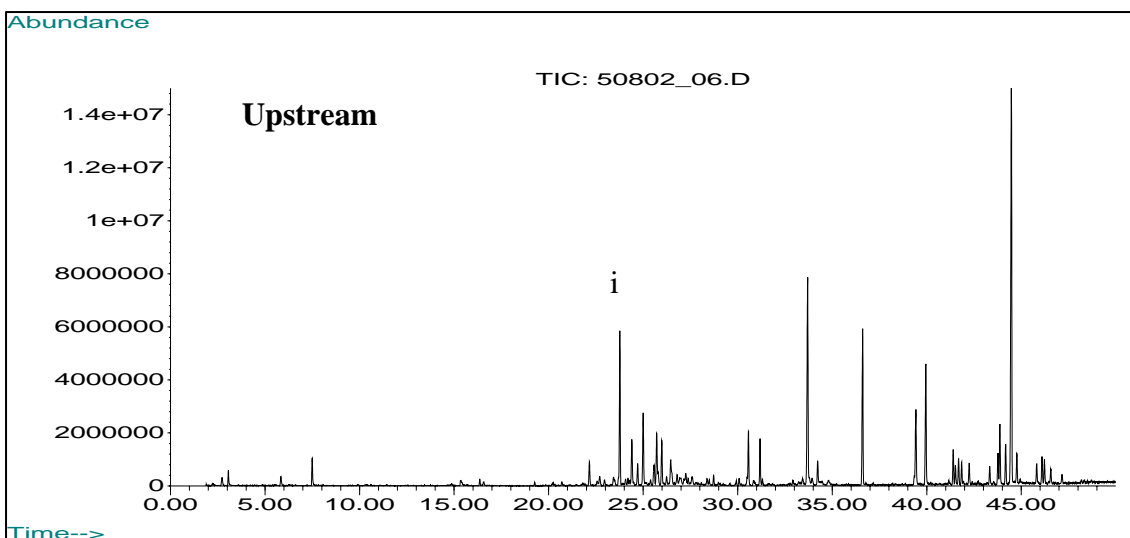


Figure 9. Comparison of total-ion-current chromatograms obtained by TD-GC/MS analysis of air samples collected upstream and downstream of UVPCO reactor in Experiment 15 with building product mixture. Production of acetone is indicated in downstream sample. a = Acetone; i = Internal standard.

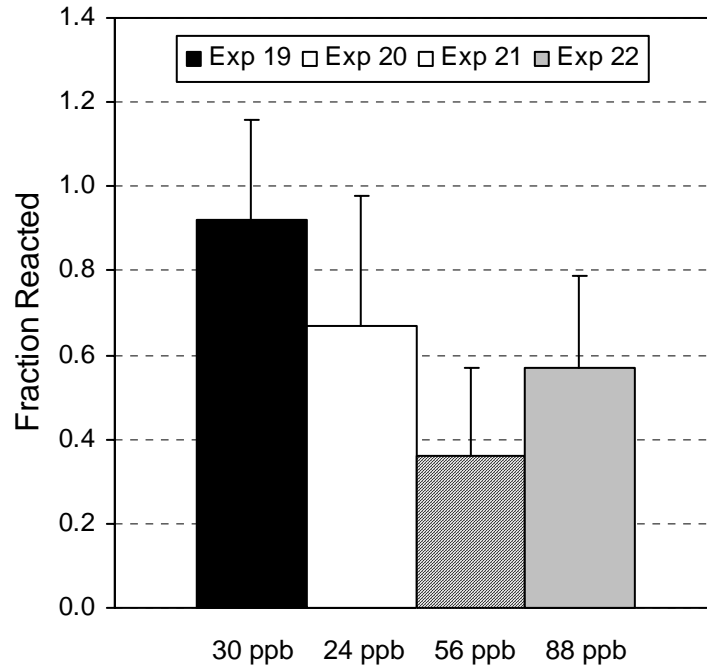


Figure 10. Mean fractions of formaldehyde reacted in experiments with aldehyde mixture in which device flow rate and the concentration of the reactants were varied. Experiment 19 was conducted at 169 m³/h; Experiments 20 – 22 were conducted at 280 – 300 m³/h. Upstream formaldehyde concentrations for Experiments 19 – 22 were 30±3, 24±3, 56±5, and 88±8 ppb, respectively. Error bars indicate two standard deviations of the means.

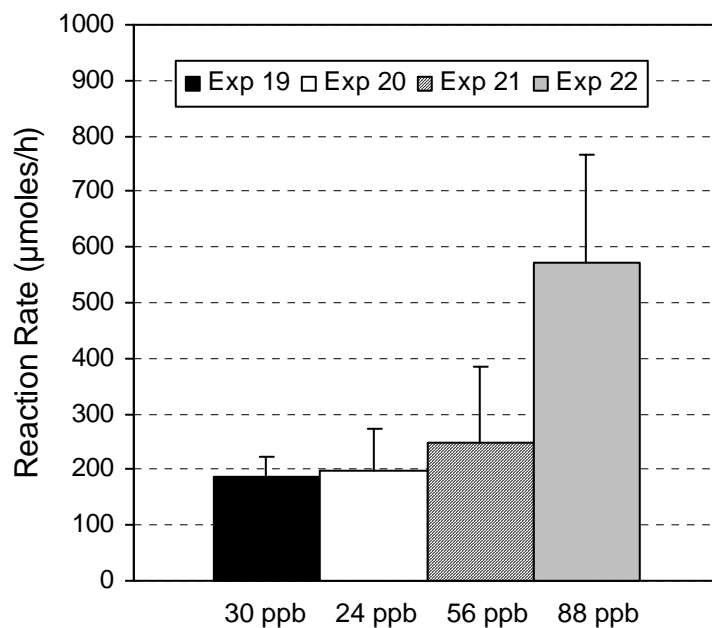


Figure 11. Mean formaldehyde reaction rates in experiments with aldehyde mixture in which device flow rate and the concentration of the reactants were varied. Experiment 19 was conducted at $169 \text{ m}^3/\text{h}$; Experiments 20 – 22 were conducted at $280 - 300 \text{ m}^3/\text{h}$. Upstream formaldehyde concentrations for Experiments 19 – 22 were 30 ± 3 , 24 ± 3 , 56 ± 5 , and 88 ± 8 ppb, respectively. Error bars indicate two standard deviations of the means.

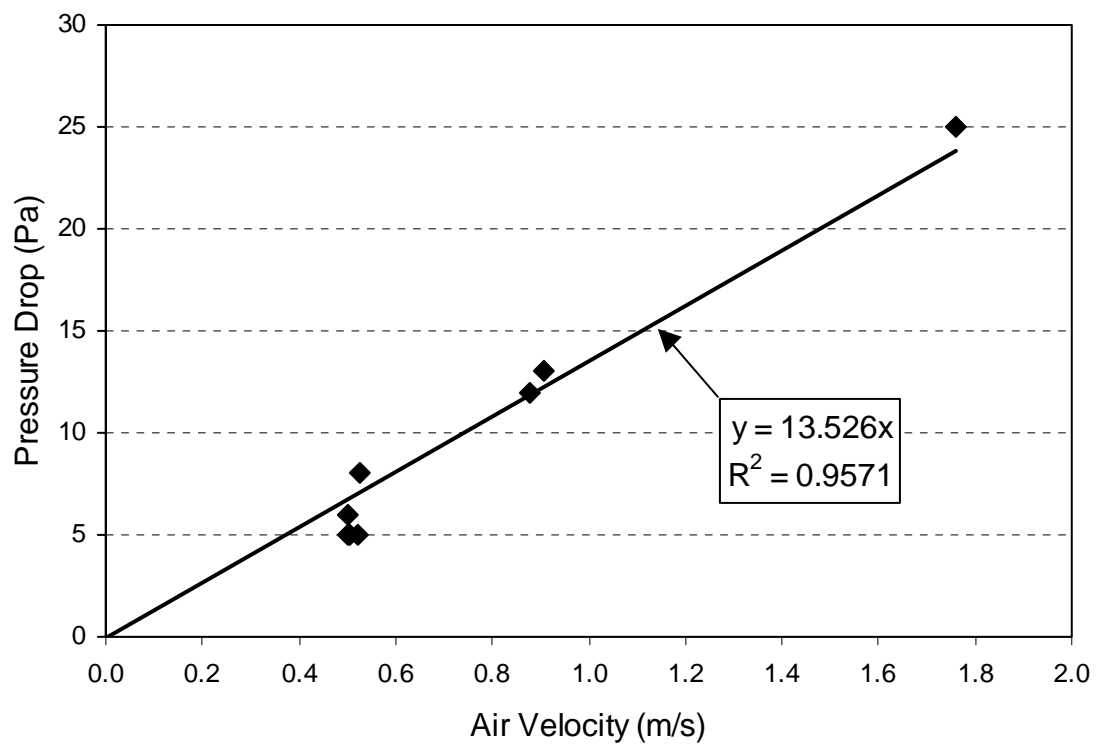


Figure 12. Pressure drop (ΔP) across the UVPCO reactor section with four 1-inch monoliths versus air velocity through the reactor.

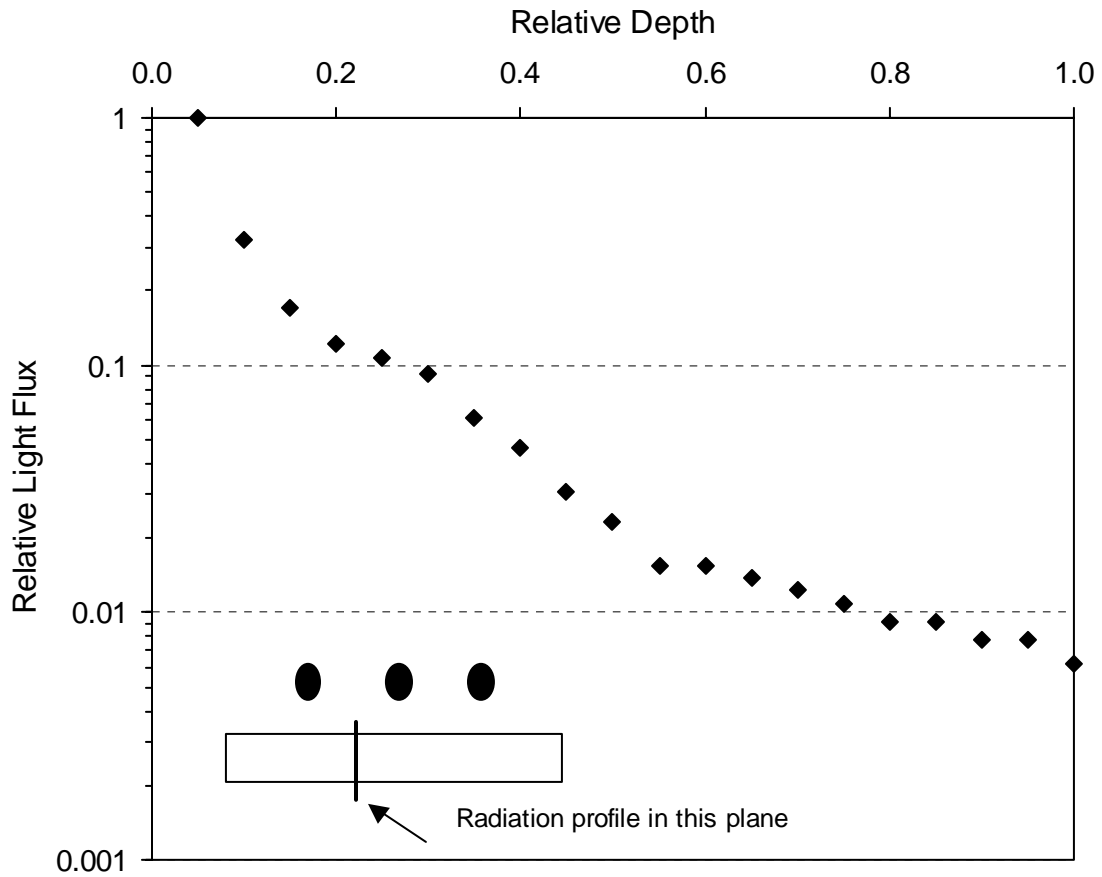


Figure 13. Predicted light intensity versus depth for a 2-in thick monolith irradiated on one face with three lamps, at a plane midpoint between an outer and the center lamp as shown in the inset diagram.

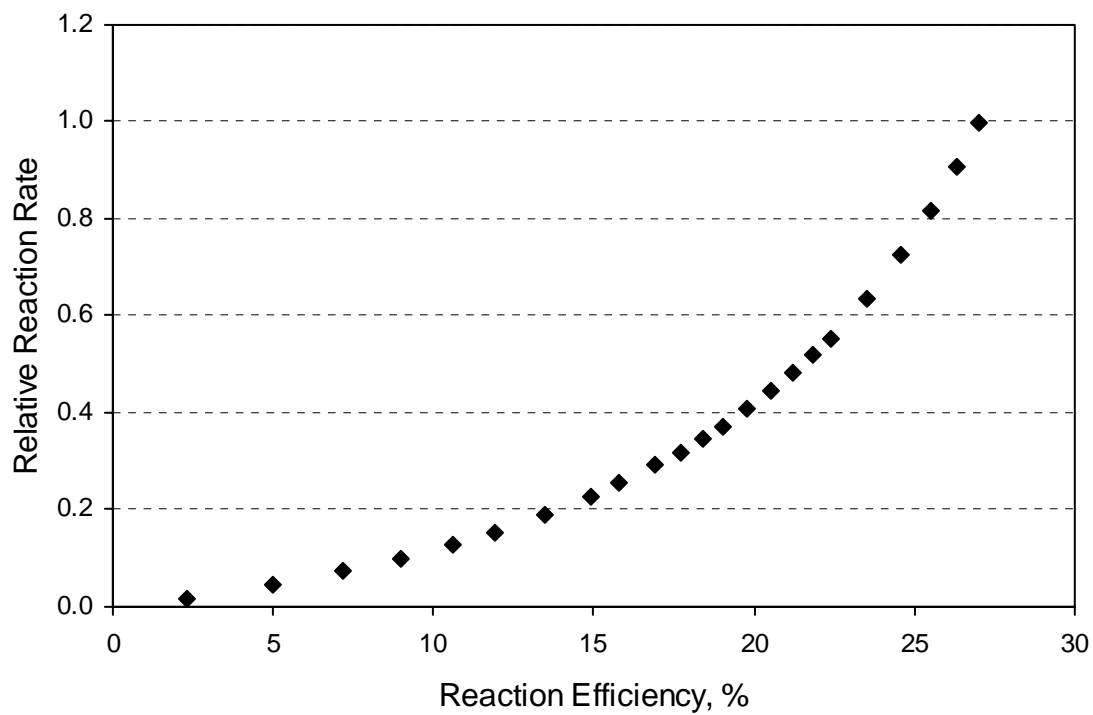


Figure 14. Predicted effect of reaction rate constant on reaction efficiency for a 1-in thick monolith irradiated on one face with three lamps and operating at 175 m³/h.